In: Ecological Modeling
Editor: WenJun Zhang, pp. 289-323
ISBN: 978-1-61324-567-5

Chapter 12

ENVIRONMENTAL NOISE AND NONLINEAR RELAXATION IN BIOLOGICAL SYSTEMS

B. Spagnolo[1*], D. Valenti[1°], S. Spezia[1], L. Curcio[2], N. Pizzolato[1], A. A. Dubkov[3], A. Fiasconaro[1,4], D. Persano Adorno[1], P. Lo Bue[5], E. Peri[5] and S. Colazza[5]

[1] Dipartimento di Fisica,
Group of Interdisciplinary Physics
Università di Palermo and CNISM, Unità di Palermo
Viale delle Scienze, ed. 18, I-90128 Palermo, Italy.
[2] Dipartimento di Ingegneria Elettrica, Elettronica e delle Telecomunicazioni,
Viale delle Scienze, ed. 9, I-90128 Palermo, Italy.
[3] Radiophysics Department, Nizhniy Novgorod State University,
23 Gagarin ave., 603950 Nizhniy Novgorod, Russia.
[4] Departamento de Fisica de la Materia Condensada, Universidad de Zaragoza,
E-50009 Zaragoza, Spain.
[5] Dipartimento di Scienze Entomologiche, Fitopatologiche,
Microbiologiche, Agrarie e Zootecniche, Università di Palermo,
Viale delle Scienze, ed. 5, I-90128 Palermo, Italy.

ABSTRACT

We analyse the effects of environmental noise in three different biological systems: (i) mating behavior of individuals of Nezara viridula (L.) (Heteroptera Pentatomidae); (ii) polymer translocation in crowded solution; (iii) an ecosystem described by a Verhulst model with a multiplicative Lévy noise. Specifically, we report on experiments on the behavioral response of N. viridula individuals to sub-threshold deterministic signals in the presence of noise. We analyze the insect response by directionality tests performed on a group of male individuals at different noise intensities. The percentage of insects which

* E-mal address: bernardo.spagnolo@unipa.it
° E-mal address: davide.valenti@unipa.it

react to the sub-threshold signal shows a nonmonotonic behavior, characterized by the presence of a maximum, for increasing values of the noise intensity. This is the signature of the non-dynamical stochastic resonance phenomenon. By using a ―hard" threshold model we find that the maximum of the signal-to-noise ratio occurs in the same range of noise intensity values for which the behavioral activation shows a maximum. In the second system, the noise driven translocation of short polymers in crowded solutions is analyzed. An improved version of the Rouse model for a flexible polymer has been adopted to mimic the molecular dynamics, by taking into account both the interactions between adjacent monomers and introducing a Lennard-Jones potential between non-adjacent beads. A bending recoil torque has also been included in our model. The polymer dynamics is simulated in a two-dimensional domain by numerically solving the Langevin equations of motion. Thermal fluctuations are taken into account by introducing a Gaussian uncorrelated noise. The mean first translocation time of the polymer center of inertia shows a minimum as a function of the frequency of the oscillating forcing field. In the third ecosystem, the transient dynamics of the Verhulst model perturbed by arbitrary non-Gaussian white noise is investigated. Based on the infinitely divisible distribution of the Lévy process we study the nonlinear relaxation of the population density for three cases of white non-Gaussian noise: (i) shot noise, (ii) noise with a probability density of increments expressed in terms of Gamma function, and (iii) Cauchy stable noise. We obtain exact results for the probability distribution of the population density in all cases, and for Cauchy stable noise the exact expression of the nonlinear relaxation time is derived. Moreover starting from an initial delta function distribution, we find a transition induced by the multiplicative Lévy noise from a trimodal probability distribution to a bimodal probability distribution in asymptotics. Finally we find a nonmonotonic behavior of the nonlinear relaxation time as a function of the Cauchy stable noise intensity.

Keywords: Stochastic resonance in Nezara viridula; Polymers translocation; Verhulst model; Stochastic processes.

1. INTRODUCTION

During last decades noise-induced effects have been experimentally observed and theoretically studied in different physical and biological contexts (Agudov and Spagnolo, 2001; Fiasconaro and Spagnolo, 2009; Spagnolo et al., 2003; Valenti et al., 2004; Spagnolo et al., 2002; Zimmer, 1999; Bjørnstad and Grenfell, 2001; Grenfell et al., 1998; Chichigina, 2008; Giuffrida et al., 2009; Korobkova et al., 2004; Pizzolato et al., 2009), such as neuronal cells, excitable systems and threshold physical systems (Braun, 1994; Moss et al., 1994; Gingl et al., 1995; Pei et al., 1995; Pikovsky, and Kurths, 1997; Nozaki and Yamamoto, 1998; Longtin and Chialvo, 1998; Stocks, 2001; Wiesenfeld et al., 1994; Gammaitoni, 1995; Wannamaker et al., 2000; Lindner et al., 2004).

In particular, stochastic resonance, resonant activation and noise enhanced stability phenomena in neuronal activation have been recently discussed (Lindner et al., 2004; Duarte et al., 2008; Prankratova et al., 2005).

Nature consists of open systems characterized by intrinsically non-linear interactions and subject to environmental noise (Spagnolo et al., 2004). The presence of random fluctuations, that are an uneliminable component of natural ecosystems, makes difficult detection and transmission of signals and can modify the information transported.

However, in the presence of some specific non-linearity of the system and for suitable intensity of noise, counterintuitive phenomena, such as stochastic resonance (SR), can be observed. This indicates that noise can play a constructive role, improving the conditions for signal detection.

SR phenomenon, initially observed in the temperature cycles of the Earth (Benzi et al., 1981), can be found in many physical and biological non-linear systems (Gammaitoni et al., 1998; Mantegna and Spagnolo, 1994; Mantegna et al., 2001; Agudov et al., 2010). SR can be modeled by a bistable potential subject to periodical driving force in the presence of external additive noise. The signature of SR is a nonmonotonic behavior, characterized by a maximum, of the signal-to-noise (SNR) ratio as a function of the noise intensity. This indicates that the noise can enhance the amplitude of deterministic signals, improving the response of the system through a resonance-like phenomenon (Moss et al., 1994; Gingl et al., 1995; Pei et al., 1995; Nozaki and Yamamoto, 1998; Longtin and Chialvo, 1998; Stocks, 2001; Wiesenfeld et al., 1994; Gammaitoni, 1995; Wannamaker et al., 2000; Lindner et al., 2004; Gammaitoni et al., 1998; Mantegna and Spagnolo, 1994; Mantegna et al., 2001; Vilar et al., 1998; Longtin et al., 1991; Bulsara et al., 1991; Chialvo and Apkarian, 1993; Neiman and Russell, 2002; Bahar et al., 2002; Douglass et al., 1993; Russell et al., 1999; Freund et al., 2002; Greenwood et al., 2000; Gailey et al., 1997). However, SR does not occur only in bistable systems, but also in monostable, excitable, and non-dynamical systems. In these situations we name this effect non-dynamical (or threshold) stochastic resonance, because the phenomenon is connected with the crossing of a threshold and can occur also in the absence of an external potential (Moss et al., 1994; Gingl et al., 1995; Vilar et al., 1998). Sensory neurons, that are threshold systems characterized by intrinsic noise, are an ideal workbench to observe non-dynamical SR (Longtin et al., 1991; Bulsara et al., 1991; Chialvo and Apkarian, 1993; Neiman and Russell, 2002; Bahar et al., 2002). Historical experiments revealed the presence of non-dynamical SR in the neural response of mechanoreceptor cells of crayfish (Douglass et al., 1993), and the improvement of sensorial activity of paddlefish in the detection of electric signals produced by preys (Russell et al., 1999; Freund et al., 2002; Greenwood et al., 2000). Such sensory neurons are ideally suited to exhibit SR as they are intrinsically noisy and operate as threshold systems (Longtin et al., 1991; Bulsara et al., 1991; Chialvo and Apkarian, 1993; Neiman and Russell, 2002; Bahar et al., 2002).

In this contribution, we study the effects of external noise in three different biological systems. We start analyzing the mating behavior of individuals of *N. viridula* (L.) (Heteroptera Pentatomidae). In particular, we investigate the role of noise in the response of male insects to mechanical vibrations emitted by female individuals and transmitted in the substrate (Čokl et al., 1999; Čokl et al., 2003; Čokl et al., 2007). *N. viridula*, the southern green stink bug, is a pentatomid insect highly polyphagous and quite harmful for agriculture (Todd, 1989; Pannizzi, 2000). *N. viridula* has up to five generations per year (Borges et al., 1987; Kiritani, 1964; Tremblay, 1981; Fucarino, 2003).

The mating behavior of *N. viridula* can be divided into long-range location and short-range courtship. The first one includes those components of the behavior that lead to the arrival of females in the vicinity of males. The long range attraction mediated by male attractant pheromone enables both sexes to reach the same plant.

Here, we analyze the mating behavior of insects during the short-range courtship, when bugs of both sexes are very close and the acoustic stimuli (improperly called songs) can be an important element in the sexual communication (Čokl et al., 1999).

The sound is produced by the tymbal, an organ sited in the back and present in adult individuals (Čokl et al., 2003). The vibrations, produced by a bug at the frequency of about *100 Hz*, propagate through the legs into the plant stem and can be detected by the vibro-receptors placed in the legs of another insect (Tremblay, 1981; Bagwell et al., 2008). Many experimental studies have been performed on this acoustic communication, analyzing the different signals characteristic of populations of *N. viridula* from Slovenia, Florida, Japan and Australia (Čokl et al., 2000).

The fundamental role of the vibratory signals suggests that a better knowledge of the mechanism of acoustic communication during the short-range courtship can help to point out more efficient strategy to control *N. viridula* populations, devising "biologic" traps whose working principle is the emission of acoustic signals. In natural conditions, *N. viridula* populations interact strongly with environment, and therefore the presence of surrounding noise becomes an essential component of the acoustic communication.

In the second part of this contribution, we consider transport phenomena of polymers in crowded solutions. In fact, the translocation of DNA and RNA across nuclear membranes as well as the crossing of potential barriers by many proteins represents a fundamental process in cellular biology. The study of the transport of macromolecules across nanometer size channels is important for both medical research in anticancer targeted therapy (Higgins, 2007; Halwachs et al., 2009) and technological applications (Mannion et al., 2006; Sundaresan et al., 2008).

First experiments on the passage of DNA molecules across an α-hemolysin (α-HL) protein channel revealed a linear relationship of the most probable crossing time τ_p with the molecule length (Kasianowicz et al., 1996). Moreover, τ_p scales as the inverse square of the temperature and the dynamics of biopolymer translocation across an α-HL channel is found to be governed by pore-molecule interactions (Akeson et al., 1999; Meller et al., 2000; Deng et al., 2003). More recent experimental studies have shown that the application of an AC voltage to drive the translocation process of DNA molecules through a nanopore plays a significant role in the DNA-nanopore interaction, and provides new insights into the DNA conformations (Deng et al., 2003; Vernier et al., 2004; Sigalov et al., 2008; Lathrop et al., 2009; Nikolaev and Gracheva, 2009).

The complex scenario of the translocation dynamics coming from experiments has been enriched by several theoretical and simulative studies (Lubensky and Nelson, 1999; Storm et al., 2005; Forrey and M. Muthukumar, 2007; Luo et al., 2008; Gracheva, and J. P. Leburton, 2008; Pizzolato et al., 2008; Panja, and G. T. Barkema, 2008; Pizzolato et al., 2009; Pizzolato et al., 2010). The mean first passage time of a Brownian particle to cross a potential barrier in the presence of thermal fluctuations and a periodic forcing field has been theoretically and experimentally investigated as a function of the driving frequency in Refs. (Doering and Gadoua, 1992; Bier and Astumian, 1993; Boguna et al., 1998; Mantegna and Spagnolo, 2000; Dubkov et al., 2004; Spagnolo et al., 2007). The translocation time of chain polymers has been theoretically studied in the presence of a dichotomically fluctuating chemical potential only as a function of its amplitude in Ref. (Park and Sung, 1998).

In particular we investigate the role of an external oscillating forcing field on the transport dynamics of short polymers surmounting a barrier, in the presence of a metastable state. We find a minimum of the mean first translocation time (MFTT) of the molecule center of mass as a function of the frequency of the forcing field. This nonlinear behavior represents the resonant activation (RA) phenomenon in polymer translocation. We find that a suitable tuned oscillating field can speed up or slow down the mean time of the translocation process of a molecule crossing a barrier, using the frequency as a control parameter. This effect can be of fundamental importance for all those experiments on cell metabolism, DNA-RNA sequencing and drug delivery mechanism in anti-cancer therapy.

In the third part of this chapter we investigate the transient dynamics of the Verhulst model perturbed by arbitrary non-Gaussian white noise. The nonlinear stochastic systems with noise excitation have attracted extensive attention and the concept of noise-induced transitions has got a wide variety of applications in physics, chemistry, and biology (Horsthemke and Lefever, 1984). Noise-induced transitions are conventionally defined in terms of changes in the number of extrema in the probability distribution of a system variable and may depend both quantitatively and qualitatively on the character of the noise, i.e. on the properties of stochastic process which describes the noise excitation. The Verhulst model, which is a cornerstone of empirical and theoretical ecology, is one of the classic examples of self-organization in many natural and artificial systems (Eigen and Schuster, 1979). This model, also known as the logistic model, is relevant to a wide range of situations including population dynamics (Horsthemke and Lefever, 1984; Morita, 1982; Ciuchi et al., 1993; Mathis and Kiffe, 1984), self-replication of macromolecules (Eigen, 1971), spread of viral epidemics (Acedo, 2006), cancer cell population (Ai et al., 2003), biological and biochemical systems (Derise and Adam, 1990; Ciuchi et al., 1996), population of photons in a single mode laser (McNeil and Walls, 1974; Ogata, 1983), autocatalytic chemical reactions (Schlögl, 1972; Chaturvedi et al., 1976; Gardiner and Chaturvedi, 1977; Bouché, 1982; Leung, 1987), freezing of supercooled liquids (Das, 1983), and social sciences (Herman and Montroll, 1972; Montroll, 1978).

By considering the season fluctuations and the random availability of resources we analyze the stochastic Verhulst equation in the presence of a non-Gaussian stochastic process. By investigating the transient dynamics of this model we obtain exact results for the mean value of the population density and its non-stationary probability distribution for different types of white non-Gaussian noise sources. Noise-induced transitions for the probability distribution of the population density and a nonmonotonic behavior of the nonlinear relaxation time as a function of the Cauchy noise intensity are found.

The chapter is organized as follows. In section 2.1 we report on experimental setup and methods used in the investigation of behavioral response in *N. viridula*. In section 2.2, we present our experimental results of directionality tests on the behavior of male individuals of *N. viridula*. In section 2.3 we discuss the experimental findings and compare them with theoretical results obtained by a hard threshold model.

In Sect. 3 we present our polymer chain model and give the details of the molecular dynamics simulation process. Results are reported in Sect. 3.1. In the next sections 4. - 6. we present our Verhulst stochastic model with Lévy noise excitation together with all the theoretical results obtained. Finally conclusions are drawn in Sect. 7.

2. BEHAVIOURAL RESPONSE IN *N. VIRIDULA*

2.1. Materials and methods

In our experiments we used individuals of *N. viridula* collected in the countryside around Palermo, and reared in laboratory conditions (Colazza et al., 2004). Male insects have been used for experimental trials after they reached sexual maturity (not less than ten days after the final moult), and a three-day period of isolation from the opposite sex (Čokl et al., 2007; Čokl et al., 2000).

The sexual calling song emitted from a female individual has been recorded by the membrane of a conic low-middle frequency loudspeaker (MONACOR SPH 165 C CARBON with a diameter of *16.5* cm). Afterwards the sound, stored on a pc, has been analyzed and processed using a commercial software. The speaker has been used as an "inverse" microphone, namely an acoustic-electric transducer: the sounds have been recorded from a low-frequency non-resonating membrane of a speaker, conveniently chosen to get a good frequency response starting at *20* Hz. The sound acquisitions have been made inside an anechoic chamber (sound insulated) at *22 - 26* °C, *70 – 80 %* of relative moisture and in presence of artificial light. The choice of this recording set-up has been decided after a comparative analysis with a recording system based on the use of a stethoscope. In particular, the speaker membrane shows greater sensitivity at medium-low frequencies, that are crucial to our experiment.

The sound has been sampled from the analogical signal source (*44100* samples per second at *16* bit) and then filtered by an 18^{th} order Tchebychev filter (type I) with band-pass from *60* to *400* Hz. This filtering has been done to cut: (i) the low frequencies due to the electric network (*50* Hz) and those from the conic loudspeaker, and (ii) the high frequencies due to the electronic apparatus. Spectral and temporal properties of the measured non-pulsed female calling songs (NPFCS) have been compared with those of North America, observing that *N. viridula* individuals collected in Sicily have the same dialect as adults of *N. viridula* collected in USA with a slightly different frequency range (Čokl et al., 2007; Čokl et al., 2000; Čokl et al., 2005).

In Fig. 1.a, the oscillogram of NPFCS is shown. The signal is characterized by a short pre-pulse followed by a longer one, according to previous experimental findings (Čokl et al., 2000). In Fig. 1.b, the power spectrum density (PSD) of NPFCS is shown. In this spectrum the dominant frequencies range from *70* to *170* Hz and the subdominant peaks do not exceed 400 Hz. The maximum peak occurs at *102.5* Hz. In Fig. 1.c we report the relative sonogram, achieved by the Short Time Fourier Transform (STFT) method. The STFT maps a signal providing information both about frequencies and occurrence times. It shows that during the first two seconds (short pre-pulse) the dominant frequency interval is narrower than the range observed in the subsequent time space. In particular in the first time interval the highest frequency does not exceed *130* Hz, whereas in the final one it reaches almost *170* Hz.

Here we study the effects of noise on the behavior of *N. viridula* during the mating period. Therefore, in order to perform directionality tests, we have designed and constructed a Y-shaped dummy plant, and placed it inside an anechoic chamber. The Y-shaped plant consists of a vertical wood stem, *10* cm long, and *0.8 - 0.9* cm thick at the top of which there are two identical wooden branches, *25* cm long, and *0.4* cm thick, as shown in Fig. 1.d. The angle between two branches is *30°* - *50°*.

In our experiment a signal is sent along one branch of the Y-shaped substrate and the behavior of single male individuals, initially placed at the center of the vertical stem, is observed [39] (see Fig. 1.d). The source of vibratory signals (i.e. the cone used as an electro-acoustic transducer) is in contact with the right apex of the Y-shaped dummy plant. Vertical stem and lateral branches are not in direct contact, albeit in close (*0.5* cm) proximity.

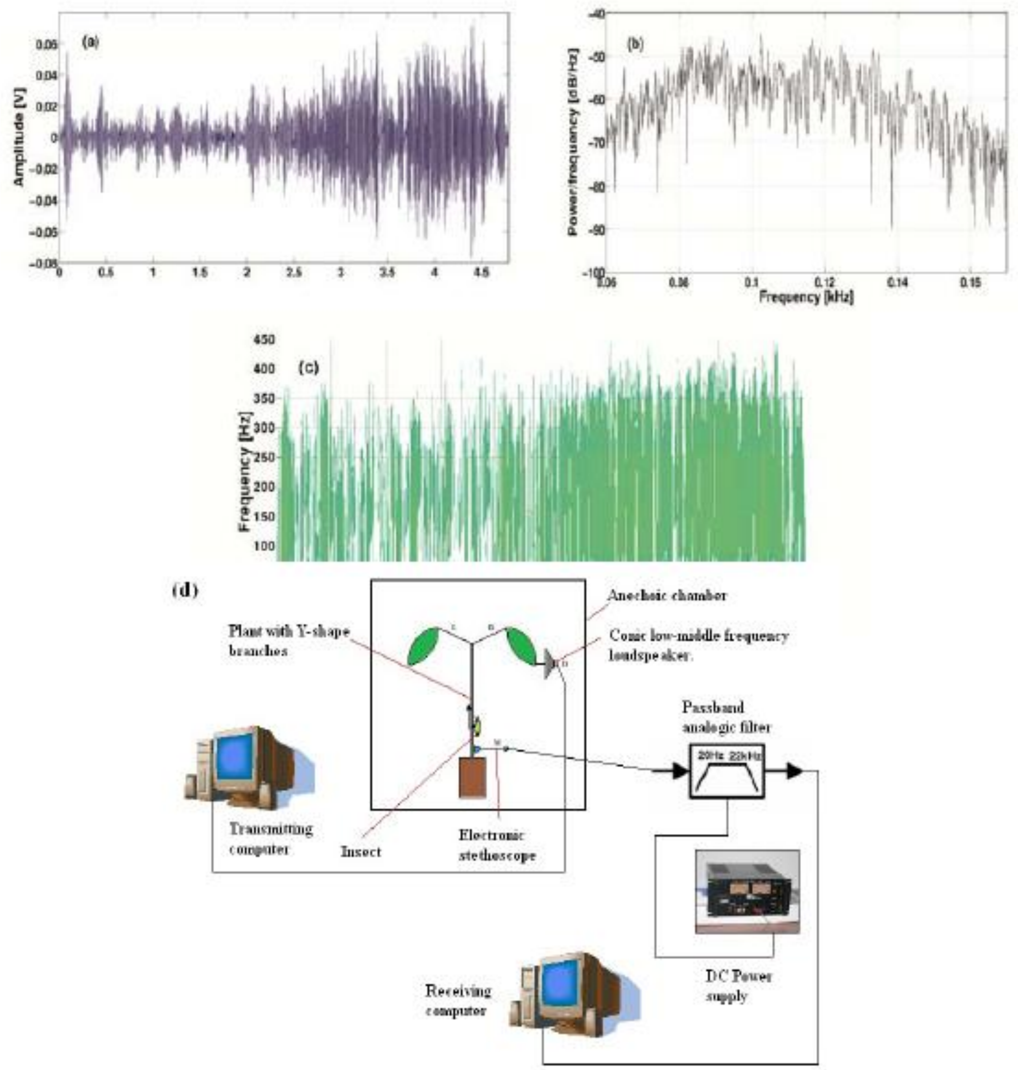

Figure 1. (a) Oscillogram (b) Power spectrum density and (c) Sonogram of the non pulsed type of *Nezara viridula* female calling song; (d) The block diagram of the experimental setup.

We consider a trial valid if the insect, before choosing one direction in the Y-shaped structure, has checked the two possible directions of signal origin, touching the lower extremity of both branches. By following these criteria, we made several observations for different intensities of female calling songs, recording the choices (left or right) of each male individual used in our trials, and obtaining a set of statistical data that allows us to determine the intensity threshold value at which the bugs start to "hear" the calling song.

2.2. Experimental Results

The presence of an "oriented" behavior, that is the tendency of the insects to choose the branch with the signal source, is revealed by performing directionality tests on a group of male individuals. When we observe a percentage of insects higher than *65%* going towards the acoustic source, *source-direction movement* (SDM), we consider that the signal has been revealed by the insects. In Fig. 2.a we plot the relative frequency of SDMs, that is the number of SDMs divided by the total trials, at different signal intensities. The exact number of trials, performed for each intensity, is reported beside the corresponding point in the graph. For small values (lower than 0.0010 V) of the signal power approximately *50%* of the insects choose one direction and the remaining 50% the other.

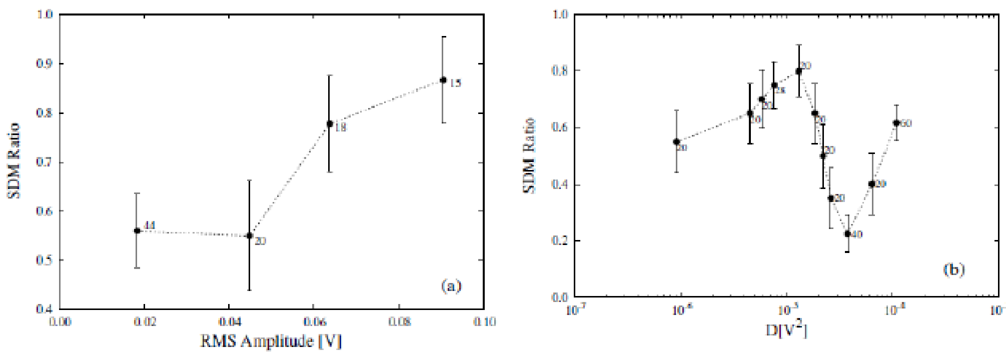

Figure 2. Plots of the *Source-Direction Movement (SDM) Ratio* as a function of: (a) the female calling song Root Mean Square (RMS) amplitude (purely deterministic signal); (b) the noise intensity *D*. In each experimental value is reported the error bar and beside the corresponding number of the performed trials.

Conversely, for values greater than 0.0020 V, the insects show a preferential behavior, choosing the direction from which the signal originates in the *80%* of the trials. Consequently, we have chosen the value 0.0015 V of the signal power as the *threshold level* for signal detection.

Then, by using a sub-threshold signal plus a Gaussian white noise signal we have investigated the response of the test insect for different levels of noise intensity *D*. In Fig. 2.b we report the percentage of SDMs as a function of *D*, finding the optimal noise intensity that maximizes the recognition between individuals of opposite sex. The graph shows a maximum for $D \approx 1.30 \cdot 10^{-5} \ V^2$. For values of *D* both lower and higher than 1.30 10^{-5} V^2, the response of insects is not significant. In particular, for $D > 1.30\ 10^{-5}\ V^2$ the percentage of individuals going towards the acoustic source decreases below 0.5 reaching 0.2 for $D \approx 3.75 \cdot 10^{-5} \ V^2$. The other values of the SDM ratio close to 50%, indicate that individuals of *N. viridula* randomly choose the direction of their motion, that is no oriented behavior occurs. The nonmonotonic behavior of SDM, with a maximum at

$D \approx 1.30 \cdot 10^{-5}$ V^2, indicates that in the presence of a sub-threshold deterministic signal, the environmental noise can play a constructive role, amplifying the weak input signal and contributing to improve the communication among individuals of *N. viridula*. The occurrence of a minimum in the SDM behavior at $D \approx 3.75 \cdot 10^{-5}$ V^2, will be subject of further investigations. A possible conjectural explanation is the following: when the noise intensity is so large that the signal received from the vibro-receptors is significantly modified, the male insects are not able to recognize the female calling song, and they exchange it for the song of some rivals.

A further increase of the noise intensity causes the spectrum of the received signal to become indistinguishable from a pure environmental noise and therefore the insect is unable to recognize any signal of *N. viridula* individuals. This implies that no significant response is observed in terms of percentage of source-direction movements (SDMs ~ 50%).

2.3. Threshold Stochastic Resonance

The presence of a maximum in the behavior of SDM percentage as a function of D can be explained either by the threshold phenomenon, or non-dynamical, stochastic resonance (TSR).

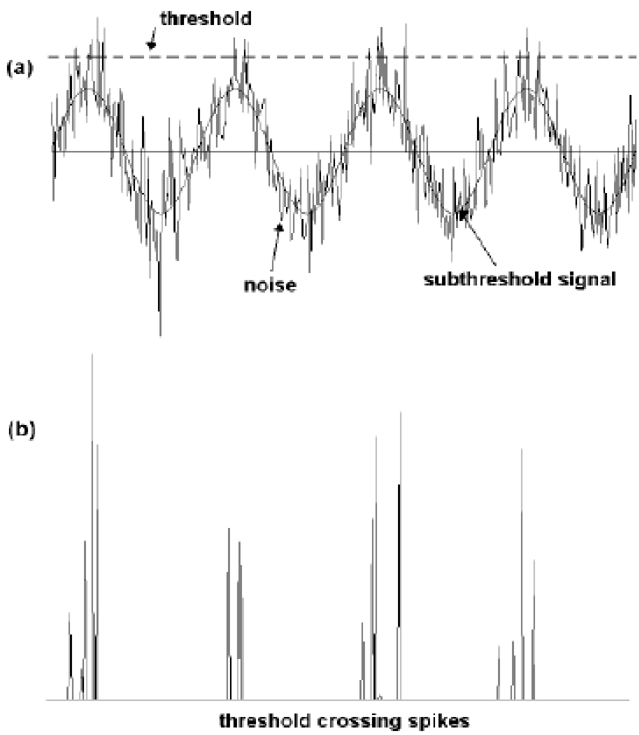

Figure 3. Evolution driven by a sinusoidal function plus noise. (a) Time series generated by consecutive pulses (dashed line: threshold level, solid line: mean value of the periodic signal); (b) Temporal sequence of threshold crossing events.

Stochastic resonance (SR), initially observed in the temperature cycles of the Earth (Benzi et al., 1981), is a counterintuitive phenomenon occurring in a large variety of non-linear systems, whereby the addition of noise to a weak periodic signal causes it to become detectable or enhances the amount of transmitted information through the system (Moss et al., 1994; Gingl et al., 1995; Pei et al., 1995; Pikovsky and Kurths, 1997; Longtin and Chialvo, 1998; Stocks, 2001; Wiesenfeld et al., 1994; Gammaitoni, 1995; Wannamaker et al., 2000; Lindner et al., 2004; Gammaitoni et al., 1998; Mantegna and Spagnolo, 1994; Mantegna et al., 2001; Vilar et al., 1998; Longtin et al., 1991; Bulsara et al., 1991; Chialvo and Apkarian, 1993; Neiman and Russell, 2002; Bahar et al., 2002; Douglass et al., 1993; Russell et al., 1999; Freund et al., 2002; Greenwood et al., 2000). When SR occurs, the response of the system undergoes resonance-like behavior as a function of the noise level. In spite of the fact that initially this phenomenon was restricted to bistable systems, it is well known that SR appears in monostable, excitable, and non-dynamical systems.

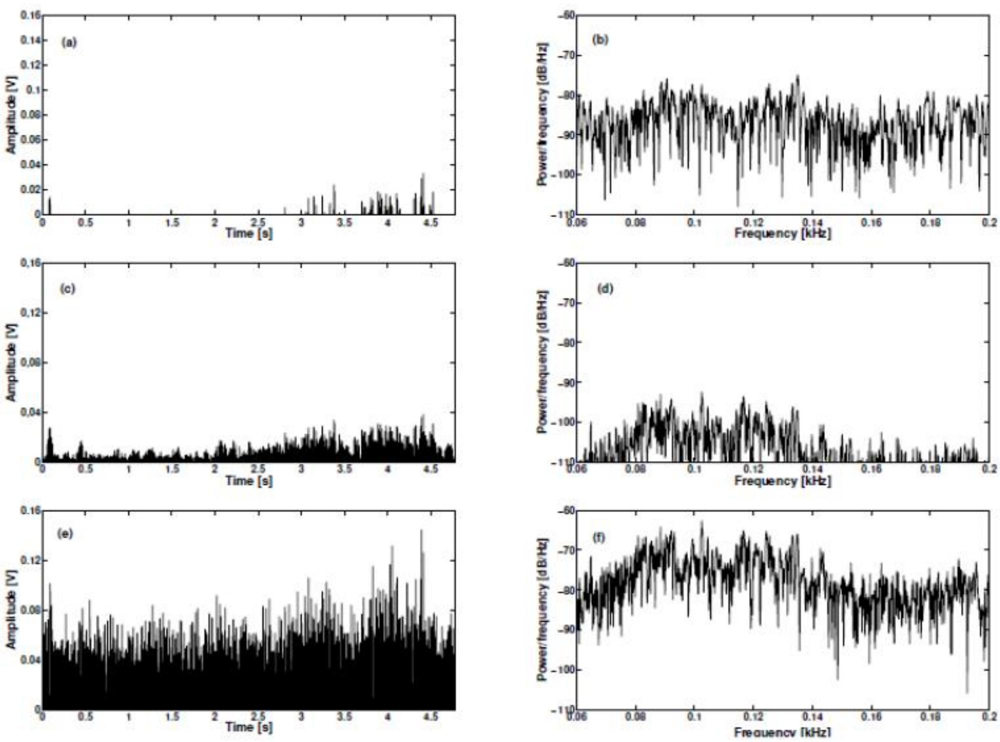

Figure 4. Temporal evolution of the simulated calling signal over the threshold for noise intensity $D = 2.6 \cdot 10^{-6}$ V^2 a), $D = 1.30 \cdot 10^{-5}$ V^2 (b) and $D = 1.0 \cdot 10^{-3}$ V^2 (c). The corresponding power spectral densities are shown in panels b, d, f. The threshold level is $s_{th} = 0.045\ V$ and RMS amplitude of the subthreshold signal is 0.031 V^2. In the figures (a), (c) and (e) we have rescaled the values of the signal amplitude in such a way that the zero value corresponds to the threshold value.

Here we report on experiments conducted on the response of *N. viridula* individuals to sub-threshold signals. The nonmonotonic behavior of SDM, as a function of the noise intensity (see Fig. 2.b), can be considered the hallmark of the threshold stochastic resonance (TSR). This phenomenon is well described by an extremely simple system, shown in Fig 3, and characterized by: (i) an energetic activation barrier (threshold); (ii) a weak coherent input such as a periodic signal (sub-threshold signal); (iii) a source of noise which is inherent to the system, or is added externally to the deterministic input (Moss et al., 1994; Gingl et al., 1995; Pei et al., 1995). Since the three ingredients are often present in nature and the idea of the existence of a threshold is quite intuitive, TSR has migrated into many different fields, so that during the last decades a considerable amount of literature on this subject has appeared in several areas of science and engineering.

We have simulated a system with a threshold 0.045 V and a subthreshold signal of RMS amplitude 0.031 V (a. u.), obtained by the recorded female calling song. In Fig. 4 we show the output signal, and the corresponding PSD, for three different levels of noise added to the subthreshold deterministic signal (calling song). In the Figs. 4.a, 4.c, 4.e we have rescaled the values of the signal amplitude in such a way that the zero value corresponds to the threshold value. For low noise intensities the signal crosses the threshold (dashed line in Fig. 4.a) very rarely, and in the corresponding PSD (Fig. 4.b) no frequency shows any significant power enhancement. By increasing the noise level the threshold crossings become more frequent (Fig. 4.c) and the PSD appears to take a larger value for f = 102.5 Hz (Fig. 4.d), that is the dominant frequency contained in the input signal. A further increase of noise intensity produces a degradation of the signal, a loss of coherence in the temporal sequence (Fig. 4.e) and a reduction of the main peak (f = *102.5 Hz*) in the PSD (Fig. 4.f). The signal-to-noise ratio (SNR) at f = 102.5 Hz is reported in Fig. 5. For each value of the noise intensity we have performed 5000 numerical realizations. The noise intensity for which the SNR is maximum is $D \approx 1.17 \cdot 10^{-5}$, which is very near the value of the noise intensity that maximizes the percentage of SDMs (see Fig. 2.b).

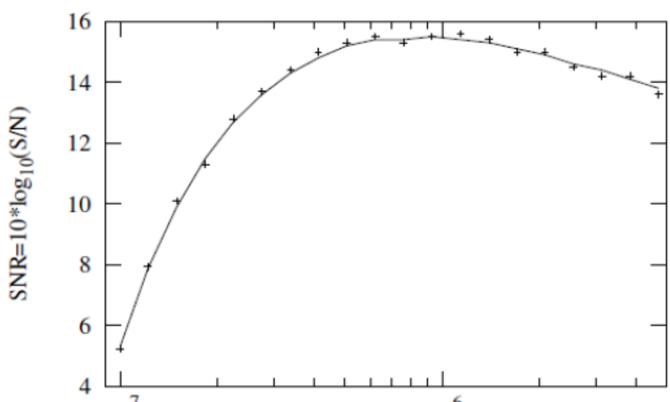

Figure 5. Signal to noise ratio versus variance noise D of the output signal model when the input female calling song is subthreshold, at the dominant frequency f = 102.5 Hz. All the other parameters are the same of Fig. 2.

The results obtained from our model suggest that in the biological system analyzed, stochastic resonance plays a key role, since it permits information to be extracted from a weak deterministic signal, thanks to the constructive action of environmental noise. In other words there is a suitable noise intensity which maximizes the activating behavior of the green bugs and this effect can be described by the simplest threshold model which shows stochastic resonance. In Fig. 5 we report also the best fitting curve of the simulations (cross points in the figure) obtained by the formula of the SNR for a single frequency coherent signal (Moss et al., 1994)

$$SNR = c \log\left[\frac{a}{D^2}\exp\left(-\frac{b}{D}\right)\right], \tag{1}$$

where $a = 6.6 \cdot 10^{-5}$, $b = 1.70 \cdot 10^{-6}$, and c = 2.18.

3. THE POLYMER CHAIN MODEL AND MD SIMULATIONS

The polymer is modeled by a semi-flexible linear chain of N beads connected by harmonic springs (Rouse, 1953). Both excluded volume effect and van der Waals interactions between all beads are kept into account by introducing a Lennard-Jones (LJ) potential. In order to confer a suitable stiffness to the chain, a bending recoil torque is included in the model, with a rest angle $\theta_0 = 0$ between two consecutive bonds. The total potential energy of the modeled chain molecule is $U = U_{Har} + U_{Bend} + U_{LJ}$ with

$$U_{\mathrm{Har}} = \sum_{i=1}^{N-1} K_{\mathrm{r}}(r_{i,i+1} - d)^2 \tag{2}$$

$$U_{\mathrm{Bend}} = \sum_{i=2}^{N-1} K_{\theta}(\theta_{i-1,i+1} - \theta_0)^2 \tag{3}$$

$$U_{\mathrm{LJ}} = 4\epsilon_{\mathrm{LJ}} \sum_{i,j(i\neq j)} \left[\left(\frac{\sigma}{r_{ij}}\right)^{12} - \left(\frac{\sigma}{r_{ij}}\right)^{6}\right]$$

where K_r is the elastic constant, r_{ij} the distance between particles i and j, d the equilibrium distance between adjacent monomers, K_θ the bending modulus, ε_{LJ} the LJ energy depth and σ the monomer diameter. The effect of temperature fluctuations on the dynamics of a chain polymer escaping from a metastable state is studied in a two-dimensional environment. The polymer translocation is modeled as a stochastic process of diffusion in the presence of a potential barrier having the form

$$U_{Ext}(x) = ax^2 - bx^3 \tag{5}$$

with parameters $a = 3 \cdot 10^{-3}$ and $b = 2 \cdot 10^{-4}$, as already adopted in Ref. (Pizzolato et al., 2009). A three-dimensional view of U_{Ext} is plotted in Fig. 6.

The drift of the i^{th} monomer of the chain molecule is described by the following overdamped Langevin equations

$$\frac{dx_i}{dt} = -\frac{\partial U_{ij}}{\partial x} - \frac{\partial U_{Ext}}{\partial x} + \sqrt{D}\,\xi_x + A\cos(\omega t + \varphi) \qquad (6)$$

$$\frac{dy_i}{dt} = -\frac{\partial U_{ij}}{\partial y} + \sqrt{D}\,\xi_y \qquad (7)$$

where U_{ij} is the interaction potential between the i^{th} and j^{th} beads, ξ_x and ξ_y are white Gaussian noise modeling the temperature fluctuations, with the usual statistical properties, namely $< \xi_x (t) > = 0$ and $< \xi_k (t) \xi_l (t+\tau) > = \delta_{kl} \delta(\tau)0$ for $(k,l = x,y)$. A and ω are respectively the amplitude and the angular frequency of the forcing field and φ a randomly chosen initial phase. In our simulations, the time t is scaled with the friction parameter γ as $t = t_r/\gamma$, where t_r is the real time of the process.

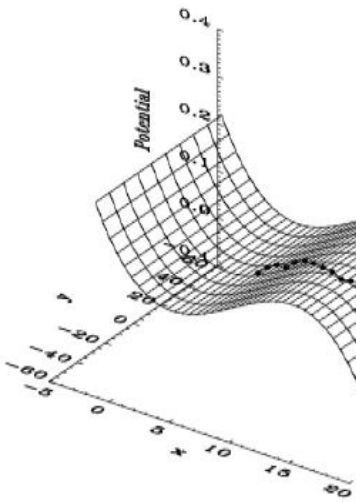

Figure 6. 3D-view of the potential energy U_{Ext} ,which is included in our system to simulate the presence of a barrier to be surmounted by the polymer. A sketch of the translocating chain molecule is shown.

The standard Lennard-Jones time scale is $\tau_{LJ} = (m\sigma^2/\varepsilon_{LJ})^{1/2}$, where m is the mass of the monomer. A bead of a single-stranded DNA is formed approximately by three nucleotide bases and then $\sigma \approx 1.5$ nm and $m \approx 936$ amu (Luo et al., 2008). Orders of magnitude of the quantities involved in the process are nanometers for the characteristic lengths of the system (polymer and barrier extension) and microseconds for the time domain. A set of 10^3 numerical simulations has been performed for different values of the frequency of the forcing field and two values of the noise intensity D, namely $D = 1.0, 4.0$. The values of the potential energy parameters are: $K_r = K_\theta = 10$, $\varepsilon_{LJ} = 0.1$, $\sigma = 3$ and $d = 5$, in arbitrary units (AU). The amplitude of the electric forcing field is $A = 5 \cdot 10^{-2}$ in AU, because it is scaled with γ. The number of monomers N is 20. The initial spatial distribution of the polymer is with all monomers at the same coordinate $x_0 = 0$, corresponding to the local minimum of the potential energy of the barrier. Every simulation stops when the x coordinate of the center of mass of the chain reaches the final position at $x_f = 15$.

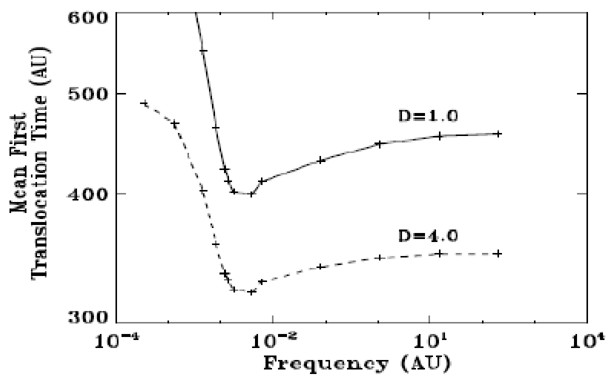

Figure 7. MFTT vs. frequency of the forcing field for two different values of the noise intensity D. The values of the potential energy parameters are: $K_r = K_\theta = 10$, $\varepsilon_{LJ} = 0.1$, $\sigma = 3$ and $d = 5$, in arbitrary units (AU). The amplitude of the electric forcing field is $A = 5 \cdot 10^{-2}$ (AU). The number of monomers N is 20.

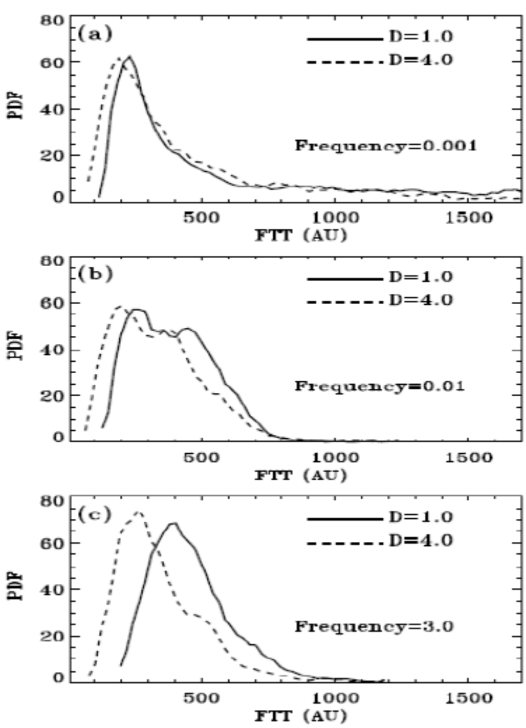

Figure 8. Probability density function (PDF) of the first translocation time (FTT). Each panel shows two PDFs, each one characterized by a specific value of the noise intensity. The three panels differs for the frequency of the forcing field. The panel (a) shows the time distribution in the low frequency region. The long tails indicate that the polymer crosses the potential barrier with a longer mean time. In the panel (b) the FTTs are distributed towards shorter values, because of the lowest time scale characterizing the translocation process in the resonant activation regime. The panel (c) shows the probability distribution for the high frequency domain, where the time scale is the same that is characterized by the presence of a static potential.

3.1. Results and Discussion

The MFTT shows three different translocation regimes as a function of the frequency (Fig. 7). In the low frequency domain ($\omega < 10^{-3}$), the period of the forcing field oscillations is very long with respect to the typical values of the mean crossing time of the chain molecule. In this regime the MFTT is equal to the average of the crossing times over upper and lower configurations of the barrier, and the slowest process determines the value of the mean crossing time. As a consequence, the MFTT increases and we observe long tails in the probability density function (PDF) shown in Fig. 8.a. In the high frequency domain ($\omega > 10^{-1}$), a saturation of the translocation time is obtained. In this case, very rapid oscillations act on the polymer motions as the mean potential, i. e. the static field, and therefore the MFTT becomes equal to that obtained without any additional periodic driving. In other words, the polymer chain feels the average potential barrier. For intermediate frequencies ($10^{-2} < \omega < 10^{-3}$), the crossing event is strongly correlated with the potential oscillations and the MFTT vs. ω exhibits a minimum at a resonant oscillation rate. This frequency region corresponds to periods of oscillations which are of the same order of magnitude of the mean time the polymer takes to cross a static barrier with its shape corresponding to the lowest configuration of the oscillating potential. In other words, the potential remains around its lowest configuration for enough time to allow the polymer to exit and, even in the case of an initially high or intermediate value of the height of the barrier, the potential feature turns into the lowest configuration within a sufficiently short time lag to facilitate the translocation process. The polymer, driven by a periodic field oscillating at a period comparable with a characteristic time of the crossing dynamics, reaches a resonant regime that accelerates the translocation process. For each of the frequency values, the thermal noise intensity D is able to speed up or slow down the crossing process, as described by the three frequency regions (Fig. 7) and the corresponding translocation dynamics (Pizzolato et al., 2010). The probability density function of the first translocation time (FTT) is shown in Fig. 8 for three frequency values characterizing the different dynamical domains. Each panel shows two PDFs, each one characterized by a specific value of the noise intensity. In the resonant activation regime (Fig. 8.b) the PDFs do not present the long tail at higher crossing times, observed in Fig. 8.a. Consequently, the MFTT reduces its value. The PDF assumes an interesting two-peaks structure that suggests the presence of two characteristic times of translocation. This feature, being present both at low and high noise intensity, can be ascribed to two different translocation dynamics of the polymer chain surmounting the barrier. In the high frequency domain (Fig. 8.c) the PDFs show the characteristic feature of the static potential case.

4. VERHULST MODEL WITH LÉVY WHITE NOISE EXCITATION

In considering how the population density $x(t)$ may change with time t, Verhulst proposed the following equation

$$\frac{dx}{dt} = rx\left(1 - \frac{x}{\Omega}\right) \tag{8}$$

where there is the Malthus term with the rate constant *r* and a saturation term with the *Ω* factor, which is the upper limit for the population growth due to the availability of the resources.

Really the parameters *r* and *Ω* are not constant. In fact the parameter *r* changes randomly due to season fluctuations, and the parameter *Ω* fluctuates due to the environmental interaction which causes the random availability of resources. As a consequence we have the following stochastic Verhulst equation

$$\frac{dx}{dt} = r(t)x\left[1 - \frac{x}{\Omega(t)}\right] \tag{9}$$

In the context of macromolecular self-replication, the model equation (9), with constant *Ω* and a white Gaussian noise in *r(t)*, was numerically studied in Ref. (Leung, 1988) and the critical slowing down, i.e. a divergence of the relaxation time at some noise intensity, was found. Later Jackson and co-authors (Jackson et al., 1989) investigated the same model, by analog experiment and digital simulations. They analyzed specifically in detail the nonlinear relaxation time defined as (Binder, 1973)

$$T = \frac{\int_0^\infty \left[\langle x(t)\rangle - \langle x(\infty)\rangle\right] dt}{x(0) - \langle x(\infty)\rangle} \tag{10}$$

and did not observe the critical slowing down. They explained this discrepancy by the incorrect approximate truncation of the asymptotic power series for *T* used in Ref. (Leung, 1988). The stability conditions were derived in Ref. (Golec and Sathananthan, 2003). Similar investigations for colored Gaussian noise *r(t)* were performed in Ref. (Mannella et al., 1990), where a monotonic dependence of the relaxation time and the correlation time on the noise intensity was found. Some exact results for Eq. (9) with constant *r* and Markovian dichotomous noise excitation $\beta(t) = r/\Omega(t)$ was obtained in Ref. (Zygadło, 2008).

The generalization of Eq. (9), to study a Bernoulli-Malthus-Verhulst model driven by a multiplicative white and colored Gaussian noise, was analyzed in Refs. (Calisto and Bologna, 2007; Suzuki et al., 1982; Brenig and N. Banai, 1982; Makino and Morita, 1985; Morita and Makino, 1986). In Refs. (Makino and Morita, 1985; Morita and Makino, 1986) the authors, using perturbation technique, obtained the exact expansion in power series on noise intensity of all the moments and found the long-time decay of $t^{-1/2}$ (see also Ref. [Ciuchi et al., 1993]).

In the present chapter, using the previously obtained results for a generalized Langevin equation with a Lévy noise source (Dubkov and Spagnolo, 2005; Dubkov et al., 2008), we investigate the transient dynamics of the stochastic Verhulst model with a fluctuating growth rate and a constant value for the saturation population density Ω, that is $\Omega = 1$. The exact results for the mean value of the population density and its non-stationary probability distribution for different types of white non-Gaussian excitation *r(t)* are obtained. We find the interesting noise-induced transitions for the probability distribution of the population density and the relaxation dynamics of its mean value for Cauchy stable noise. Finally we obtain a nonmonotonic behavior of the nonlinear relaxation time as a function of the Cauchy noise intensity.

5. Stochastic Verhulst Equation with Non-Gaussian Fluctuations of Growth Rate

Let us consider Eq. (9) with a constant saturation value $\Omega = 1$, namely

$$\frac{dx}{dt} = r(t)x(1-x). \tag{11}$$

After changing variable $y = ln[x/(1-x)]$, we obtain

$$y(t) = y(0) + \int_0^t r(\tau)\, d\tau$$

and the exact solution of Eq. (11) is

$$x(t) = \left(1 + \frac{1-x_0}{x_0} \exp\left\{-\int_0^t r(\tau)\, d\tau\right\}\right)^{-1}, \tag{12}$$

where $x_0 = x(0)$. Now by substituting in Eq. (12) the following expression for the random rate $r(t)$

$$r(t) = r + \xi(t), \tag{13}$$

Where $r > 0$ and $\xi(t)$ is an arbitrary white non-Gaussian noise with zero mean, we can rewrite the solution (12) as

$$x(t) = \left(1 + \frac{1-x_0}{x_0} e^{-rt - L(t)}\right)^{-1}. \tag{14}$$

Here $L(t)$ denotes the so-called Lévy random process with $L(0) = 0$, and $\xi(t) = \dot{L}(t)$. As it was shown in Refs. (Dubkov and Spagnolo, 2005; Dubkov et al., 2008; Feller, 1971), Lévy process having stationary and statistically independent increments on non-overlapping time intervals belongs to the class of stochastic processes with infinitely divisible distributions. As a consequence, the characteristic function of $L(t)$ can be represented in the following form (see Eq. (6) in [Dubkov and Spagnolo, 2005])

$$\left\langle e^{iuL(t)} \right\rangle = \exp\left\{ t \int_{-\infty}^{+\infty} \frac{e^{iuz} - 1 - iu\sin z}{z^2} \rho(z)\, dz \right\}, \tag{15}$$

where $\rho(z)$ is some non-negative kernel function. The case $\rho(z) = 2D\delta(z)$ corresponds to a white Gaussian noise excitation $\xi(t)$, while for a symmetric Lévy stable noise $\xi(t)$ with index α we have a power-law kernel $\rho(z) = Q|z|^{1-\alpha}$, with $0<\alpha<2$.

In the model under consideration the stationary probability distribution has; (i) a singularity at the stable point $x = 1$ for white Gaussian noise; and (ii) two singularities at both stable points $x = 0$ and $x = 1$ for Lévy noise. To analyze the time behavior of the probability distribution in the transient dynamics it is better not to use the Kolmogorov equation for the probability density $P(x,t)$, but rather the exact solution (14). Using the standard theorem of the probability theory regarding a nonlinear transformation of a random variable, we find from Eq. (14)

$$P(x,t) = \frac{1}{x(1-x)} P_L\left(\ln\left[\frac{(1-x_0)x}{x_0(1-x)} \right] - rt, t, \right) \tag{16}$$

where $P_L(z,t)$ is the probability density corresponding to the characteristic function (15). For a white Gaussian noise $\xi(t)$, this distribution reads

$$P_L(z,t) = \frac{1}{2\sqrt{\pi D t}} \exp\left\{ -\frac{z^2}{4Dt} \right\}. \tag{17}$$

The time evolution of the probability distribution $P(x,t)$ for $D = 0.3$, $r = 2$, and $x_0 = 0.1$ is plotted in Fig. 9.

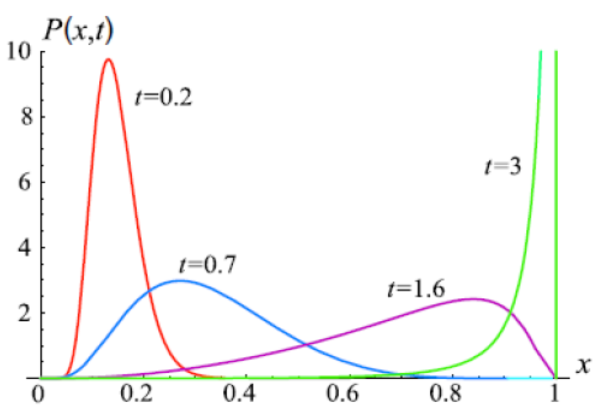

Figure 9. Time evolution of the probability distribution of the population density for white Gaussian noise excitation with intensity D. The values of the parameters are: $x_0 = 0.1$, $r = 2$, $D = 0.3$.

As it is easily seen, the maximum of the unimodal distribution with initial position at $x_0 = 0.1$ shifts with time towards the stable point at $x = 0.1$. At the same time, as it follows from Eqs. (16) and (17), for all $t > 0$ we have

$$\lim_{x \to 0^+} P(x,t) = \lim_{x \to 1^-} P(x,t) = 0. \tag{18}$$

The same picture is observed for another kernel function $\rho(z) = Kz/(2\sinh z) \quad (K > 0)$, corresponding to a Lévy process $L(t)$ with finite moments and the following probability density of increments

$$P_L(z,t) = \frac{2^{Kt-1}}{\pi^2 \Gamma(Kt)} \Gamma\left(\frac{Kt}{2} + \frac{iz}{\pi}\right) \Gamma\left(\frac{Kt}{2} - \frac{iz}{\pi}\right) \tag{19}$$

where $\Gamma(x)$ is the Gamma function. The corresponding time evolution of the probability distribution $P(x,t)$ for $K = 0.2$, $r = 2$, and $x_0 = 0.1$ is shown in Fig. 10.

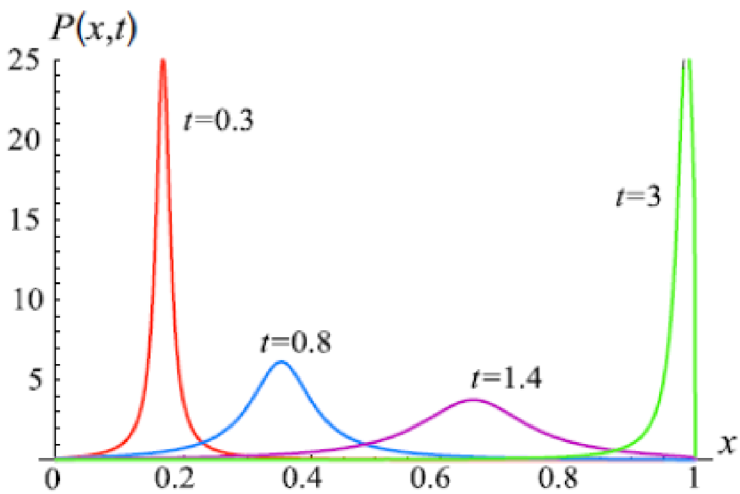

Figure 10. Time evolution of the probability distribution of the population density in the case of Lévy noise with distribution (19). The values of the parameters are: $x_0 = 0.1$, $r = 2$, $K = 0.2$.

A different situation we have for a Cauchy stable noise $\xi(t)$ with constant kernel $\rho(z) = Q \quad (\alpha = 1)$. After evaluation of the integral in Eq. (15), the probability density of the Lévy process increments takes the form of the well-known Cauchy distribution (Feller, 1971)

$$P_L(z,t) = \frac{D_1 t}{\pi \left[z^2 + (D_1 t)^2\right]}, \tag{20}$$

where $D_1 = \pi Q$ is the noise intensity parameter. In such a case from Eqs. (16) and (20) for all $t > 0$ we find

$$\lim_{x \to 0^+} P(x,t) = \lim_{x \to 1^-} P(x,t) = \infty. \tag{21}$$

As a result, from an initial delta function we immediately obtain a trimodal distribution for $t > 0$ and then after some transition time t_c a bimodal one with two singularities at the stable points $x = 0$ and $x = 1$ (see Figs. 11 - 13).

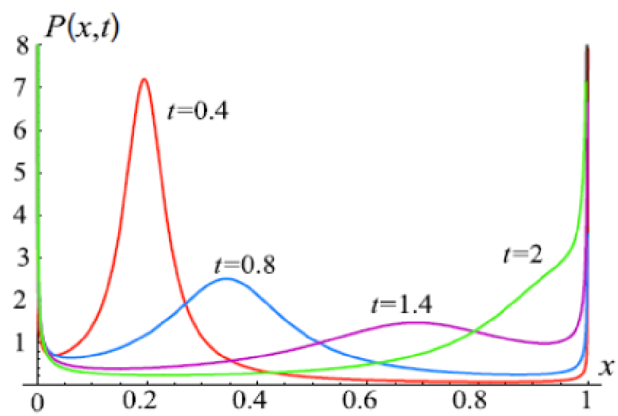

Figure 11. Time evolution of the probability distribution of the population density in the case of white Cauchy noise excitation. The values of the parameters are: $x_0 = 0.1$, $r = 2$, $D_1 = 0.7$.

We should note that the transition from trimodal to bimodal distribution is a general feature of the model in the presence of a Cauchy stable noise, and it is not limited to some range of parameters. In fact, from Eq. (21) and a delta function initial distribution inside the interval *(0,1)*, this transition always takes place.

In the following Figs. 12 and 13 we show the time evolution of the probability distribution of the population density for two other values of the noise intensity, namely $D_1 = 1.2$ and $D_1 = 1.7$. As the noise intensity increases the probability distribution shows two singularities near $x = 0$ and $x = 1$ with different amplitude.

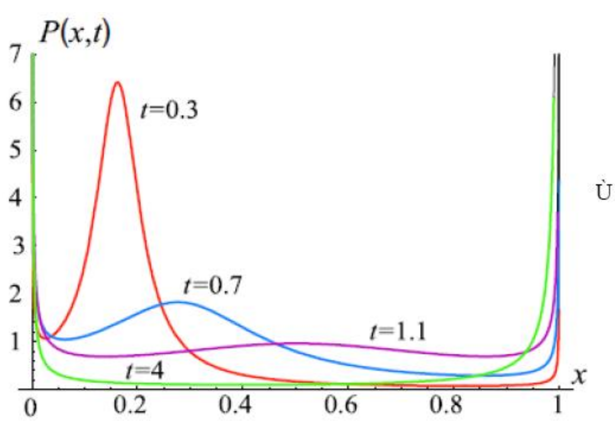

Figure 12. Time eolution of the probability distribution of the population density in the case of white Cauchy noise. The values of the parameters are : $x_0 = 0.1$, $r = 2$, $D_1 = 1.2$.

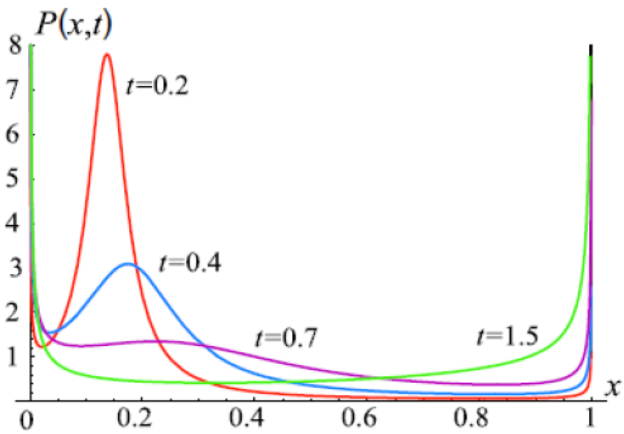

Figure 13. Time evolution of the probability distribution of the population density in the case of white Cauchy noise. The values of the parameters are $x_0 = 0.1$, $r = 2$, $D_1 = 1.7$.

This transition in the shape of the probability distribution of the population density is due to both the multiplicative noise and the Lévy noise source. Using Eqs. (16) and (20) and equating to zero the derivative of $P(x,t)$ with respect to x, we obtain the following condition for the extrema in the range $0 < x < 1$, and particularly for a minimum in the same interval

$$\frac{z(x,t)}{z(x,t)^2 + (D_1 t)^2} = x - \frac{1}{2}\ , \tag{22}$$

with

$$z(x,t) = \ln\left[\frac{(1-x_0)x}{x_0(1-x)}\right] - rt\ . \tag{23}$$

This condition can be solved graphically by finding the intersection between the functions $y_1 = z(x,t)/(z(x,t)^2 + (D_1 t)^2)$ and $y_2 = x - 1/2$. This is done in the following Figs. 14 - 16, where the function y_1 is plotted for three different values of time and noise intensity. In each figure the black blue curve (color on line) corresponds to the critical value of time t_c for which we have a noise induced transition of the probability distribution of the population density from trimodal to bimodal, that is from two minima and one maximum to one minimum inside the interval $0 < x < 1$. The appearance of one minimum in the probability distribution is the signature of this transition.

The three values of the critical time t_c corresponding to the three values of the Lévy noise intensity investigated are: $(D_1)_1 = 0.7, t_c = 1.75$; $(D_1)_2 = 1.2, t_c = 1.3$; $(D_1)_1 = 1.7, t_c = 0.95$. One rough evaluation of the critical time t_c is obtained by putting equal to 1 the scale parameter of the Cauchy distribution of Eq. (20), that is $1/D_1$. The critical time t_c is the time at which the maximum and one minimum of the probability distribution (see Figs. 11 - 13) coalesce in one inflection point and in this point x the function $y_2 = x - 1/2$ becomes tangent at the function y_1 (see Figs. 14 - 16). It is interesting to note that the critical time t_c decreases with the noise intensity D_1. This is because by increasing the noise intensity, more quickly the population density reaches the two points near the boundaries $x = 0$ and $x = 0$.

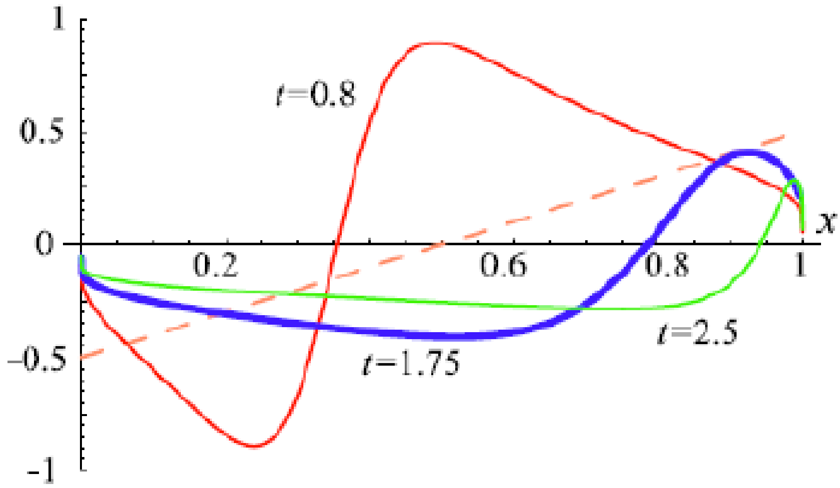

Figure 14. Plots of both sides of Eq. (22) (white Cauchy noise): function y_1 (solid curves), function y_2 (dashed curve), for three values of time, namely: $t = 0.8, 1.75, 2.5$. The critical time is $t_c = 1.75$ (black blue curve). The values of the other parameters are: $x_0 = 0.1$, $r = 2$, $D_1 = 0.7$.

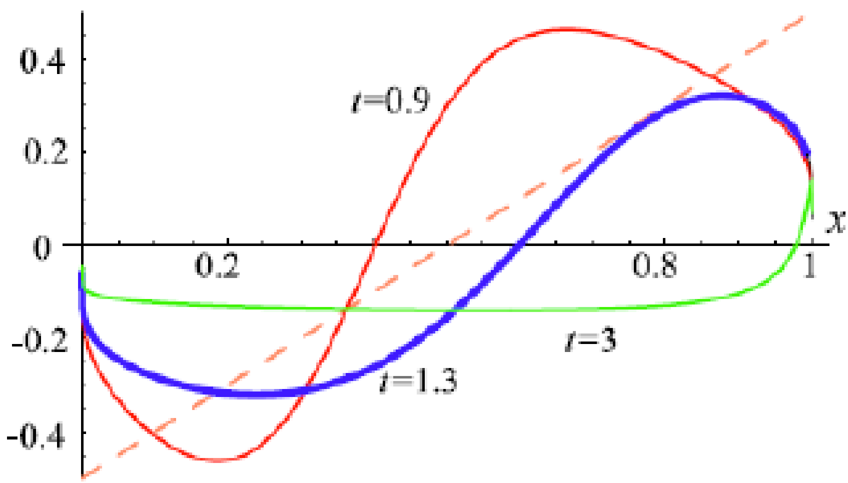

Figure 15. Plots of both sides of Eq. (22) (white Cauchy noise): function y_1 (solid curves), function y_2 (dashed curve), for three values of time, namely: $t = 0.9, 1.3, 3$. The critical time is $t_c = 1.3$ (black blue curve). The values of the other parameters are: $x_0 = 0.1$, $r = 2$, $D_1 = 1.2$.

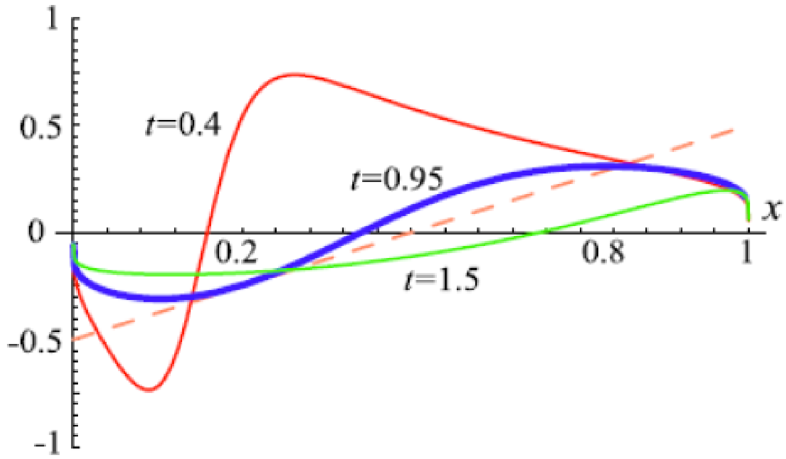

Figure 16. Plots of both sides of Eq. (22) (white Cauchy noise): function y_1 (solid curves), function y_2 (dashed curve), for three values of time, namely: $t = 0.4, 0.95, 1.5$. The critical time is $t_c = 0.95$ (black blue curve). The values of the other parameters are: $x_0 = 0.1$, $r = 2$, $D_1 = 1.7$.

6. Nonlinear Relaxation Time of the Mean Population Density

It must be emphasized that to find the time evolution of the mean population density one can use two different approaches. The first one was proposed in Ref. (Jackson et al., 1989). According to the exact solution (14) of the Verhulst equation (11), we can rewrite this expression in the following form

$$x(t) = f\left(e^{-rt-L(t)}\right), \tag{24}$$

where

$$f(q) = \left(1 + \frac{1-x_0}{x_0} q\right)^{-1}. \tag{25}$$

Then, by expanding the smooth function (25) in a standard Taylor power series in q around the point $q = 0$ we have

$$f(q) = \sum_{n=0}^{\infty} \frac{f^{(n)}(0)}{n!} q^n. \tag{26}$$

After substitution of Eq. (26) in (24) and averaging we obtain

$$\langle x(t)\rangle = \sum_{n=0}^{\infty} \frac{f^{(n)}(0)\, e^{-nrt}}{n!} \left\langle e^{-nL(t)} \right\rangle \tag{27}$$

or, in accordance with Eq. (15),

$$\langle x(t)\rangle = \sum_{n=0}^{\infty} \frac{f^{(n)}(0)\, e^{-nrt}}{n!} \exp\left\{ t \int_{-\infty}^{+\infty} \frac{e^{-nz} - 1 + n\sin z}{z^2} \rho(z)\, dz \right\}. \tag{28}$$

For white Gaussian noise $\xi(t)$ with kernel $\rho(z) = 2\,D\,\delta(z)$ we obtain from Eq. (28) the following asymptotic series

$$\langle x(t)\rangle = \sum_{n=0}^{\infty} \frac{f^{(n)}(0)}{n!}\, e^{Dtn^2 - nrt}. \tag{29}$$

By considering a finite number of terms in this expansion leads to a wrong conclusion about the critical slowing down phenomenon in such a system, as found in Ref. (Leung, 1988). The exact result is obtained, of course, by summing all the terms in Eq. (29). Moreover, for most of the kernels $\rho(z)$ the integral in Eq. (28) diverges. Thus, this approach is inappropriate for our purposes, and it is better to use the direct averaging in Eq. (14). Therefore, using this second approach we have

$$\langle x(t)\rangle = \int_{-\infty}^{+\infty} \left(1 + \frac{1 - x_0}{x_0}\, e^{-rt-z}\right)^{-1} P_L(z,t)\, dz. \tag{30}$$

Let us consider now different models of white non-Gaussian noise $\xi(t)$.

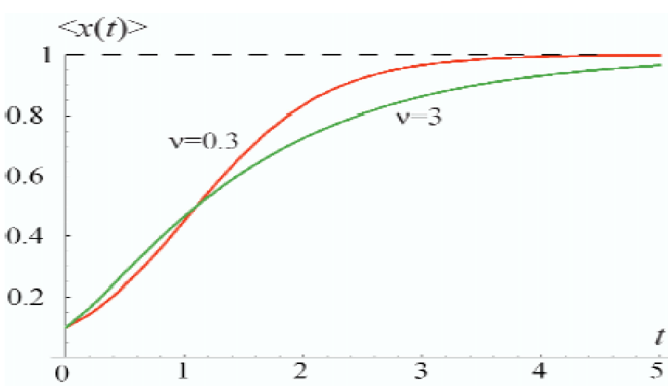

Figure 17. Nonlinear relaxation of the mean population density in the case of white shot noise excitation, for three values of the mean frequency ν, namely $\nu = 0.3$, 3. The values of the other parameters are: $x_0 = 0.1$, $r = 2$, $a_0 = 1$.

We start with the white shot noise

$$a_i \delta (t - t_i) \tag{31}$$

having the symmetric dichotomous distribution of the pulse amplitude $P(a) = [\delta (a - a_0) + \delta (a + a_0)]/2$, the mean frequency ν of pulse train, and the kernel $\rho (z) = \nu z^2 P(z)$. From Eq. (15) we have

$$\langle e^{iuL(t)} \rangle = e^{-\nu t (1 - \cos a_0 u)}. \tag{32}$$

By making the reverse Fourier transform in Eq. (32) we find the probability distribution of the corresponding Lévy process

$$P_L(z,t) = e^{-\nu t} \sum_{n=-\infty}^{+\infty} I_n(\nu t)\, \delta (z - n a_0)\,, \tag{33}$$

where $I_n(x)$ is the *n*-order modified Bessel function of the first kind. The relaxation of the mean population density $<x(t)>$ is shown in Fig. 17. According to the Eqs. (30) and (33) the stationary value of the population density in such a case is $<x(t)>_{st} = 1$, but the relaxation time (10) increases with increasing the mean frequency of pulses.

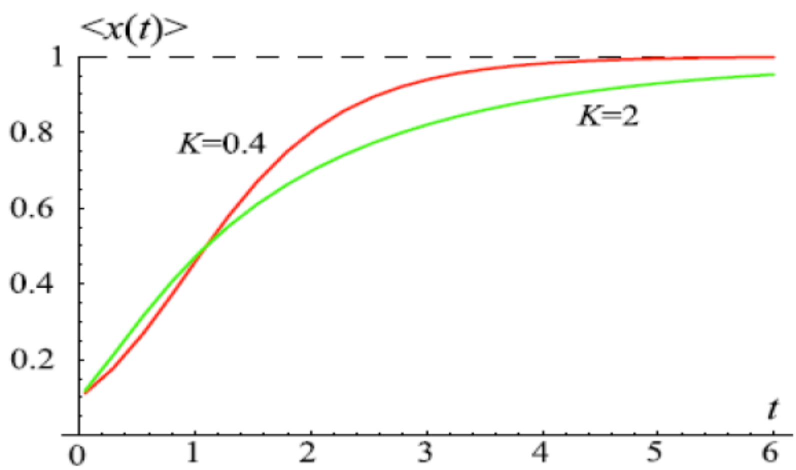

Figure 18. Nonlinear relaxation of the mean population density in the case of Lévy noise with distribution (19), for three values of the parameter *K*, namely $K = 0.4, 2$. The values of the other parameters are: $x_0 = 0.1$, $r = 2$.

For white non-Gaussian noise with the kernel $\rho(z) = Kz/(2\sinh z)$ we observe a similar transient dynamics, which is shown in Fig. 16. We have the same stationary value $<x(t)>_{st}$, and the relaxation time *T* increases with increasing the parameter *K*, which is proportional to the noise intensity. Finally, in the case of white Cauchy noise $\xi(t)$ we obtain interesting exact analytical results. First of all, substituting Eq. (20) in (30) and changing the variable $z = D_1 t y$ under the integral, we obtain

$$\langle x(t)\rangle = \frac{1}{\pi}\int_{-\infty}^{+\infty}\left[1+\frac{1-x_0}{x_0}e^{-t(r+D_1 y)}\right]^{-1}\frac{dy}{1+y^2}. \quad (34)$$

For the stationary mean value $<x(t)>_{st}$ we find from Eq. (34)

$$\langle x\rangle_{st} = \lim_{t\to\infty}\langle x(t)\rangle = \frac{1}{\pi}\int_{-\infty}^{+\infty}\frac{1(r+D_1 y)\,dy}{1+y^2}, \quad (35)$$

where $1(x)$ is the step function. After evaluation of the integral in Eq. (35) we obtain finally

$$\langle x\rangle_{st} = \frac{1}{2}+\frac{1}{\pi}\arctan\frac{r}{D_1}. \quad (36)$$

As it is seen from Fig. 19 and Eq. (36), for small noise intensity D_1, with respect to the value of the rate parameter $r = 2$, the stationary mean value of the population density is approximately 1, as for the other white non-Gaussian noise excitations considered. But for large values of D_1, this asymptotic value, which is independent from the initial value of population density x_0, tends to 0.5.

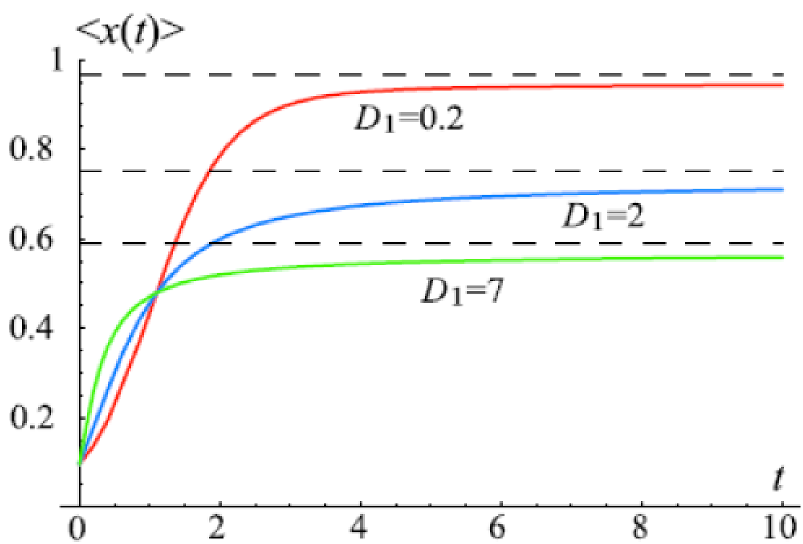

Figure 19. Nonlinear relaxation of the mean population density in the case of white Cauchy noise, for three values of the noise intensity D_1, namely $D_1 = 0.2,2,7$. The values of the other parameters are: $x_0 = 0.1$, $r = 2$.

It is interesting also to analyze, for this case of white Cauchy noise, the dependence of the relaxation time T from the noise intensity D_1. Substituting Eq. (34) in (10) and changing the order of integration, for initial condition $x_0 = 0.5$, we are able to calculate analytically the double integral in t and in y obtaining the final result

$$T = \frac{\pi \ln 2}{r\left(1 + D_1^2/r^2\right)\operatorname{arccot}(D_1/r)}. \qquad (37)$$

We find a nonmonotonic behavior of the relaxation time T versus the noise intensity D_1 with a maximum at the noise intensity D_1 = 0.75, as shown in Fig. 20.

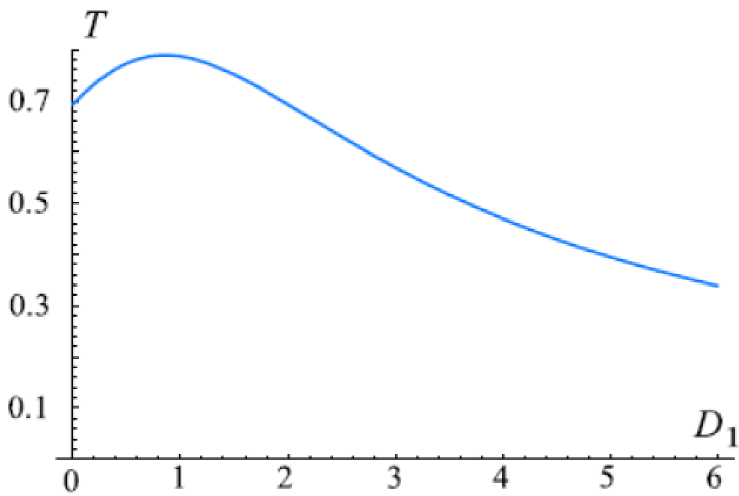

Figure 20. Nonmonotonic behavior of the nonlinear relaxation time T as a function of the white Cauchy noise intensity D_1. The values of the other parameters are: : $x_0 = 0.5$, $r = 2$.

This nonmonotonic behavior is also visible for another initial position: $x_0 = 0.1$ in Fig. 19. Here the relaxation time to reach the stationary value of mean population density $\langle x(t)\rangle_{st}$, increases from very low noise intensity ($D_1 = 0.2$) to moderate low intensity ($D_1 = 2$), while decreases for higher noise intensities ($D_1 = 7$). This is also due to the dependence of $\langle x(t)\rangle_{st}$ from the noise intensity D_1 (see Eq. (36)). We note that this nonmonotonic behavior of the relaxation time T is related to the peculiarities of the transient dynamics of the mean population density and it will be object of further investigations.

CONCLUSIONS

In this contribution we have studied the effects of random fluctuations, i.e. noise, in the vibrational communications occurring during the mating of *N. viridula*, i.e. the green bug. In our experimental work we analyzed the behavioral response of different individuals of *N. viridula* to a deterministic signal (calling song), measuring for these individuals the threshold of the neural activation. Afterwards, we analyzed the green bug response when a sub-threshold deterministic signal is added with an external noise source. By using the *Source-Direction Movement ratio* as indicator of positive response to the external signal, we observe that the behavioral activation of the insects is characterized by a nonmonotonic behavior as a function of the noise intensity D, with a maximum at $D = D_{opt} \approx 1.30 \cdot 10^{-5} \quad V^2$. The value D_{opt} maximizes the efficiency of the sexual communication among individuals of *Nezara viridula (L.)*, and therefore represents the optimal noise intensity during the mating behavior of these insects. The nonmonotonic behavior observed in the insect response as a function of the noise intensity is the signature of the threshold stochastic resonance (TSR) [117]. By using a threshold model we obtained numerical results for the threshold crossing, which corresponds in our model to the behavioral activation, finding a theoretical value for the optimal noise intensity. Experimental and numerical results are compared, finding a good agreement between the values of the optimal noise intensity obtained by the experimental work and model (see Figs. 2.2(b) and 3).

We analyzed the influence of an external oscillating driving field on the translocation dynamics of short polymers embedded in a noisy environment. We simulate the translocation process by letting the polymer to cross a potential barrier starting from a metastable state, in the presence of thermal fluctuations. The mean translocation time as a function of the frequency of the driving force shows a nonmonotonic behavior, with the noise intensity acting as a scaling factor of the values of the crossing times. The forcing periodic electric field jointly with the temperature of the system can be able to speed up or slow down the polymer translocation. In this view, the oscillating electric field constitutes a tuning mechanism to select a suitable translocation time of the polymer. This feature may have important biological effects on the cell metabolism, for example, during a cancer targeted therapy.

Finally, the transient dynamics of the Verhulst model, perturbed by arbitrary non-Gaussian white noise, has been investigated. This well-known equation is an appropriate ecological and biological model to describe closed-population dynamics, self-replication of macromolecules under constraint, cancer growth, spread of viral epidemics, etc... By using the properties of the infinitely divisible distribution of the generalized Wiener process, we analyzed the effect of different non-Gaussian white sources on the nonlinear relaxation of the mean population density and on the time evolution of the probability distribution of the population density. We obtain exact results for the non-stationary probability distribution in all cases investigated and for the Cauchy stable noise we derive the exact analytical expression of the nonlinear relaxation time. Due to the presence of a Lévy multiplicative noise, the probability distribution of the population density exhibits a transition from a trimodal to a bimodal distribution in asymptotics. This transition, characterized by the appearance of a minimum, happens at a critical time t_c, which can be roughly evaluated as $1/D_1$ (where D_1 is the noise intensity) and exactly evaluated from the condition (22). Finally a nonmonotonic behavior of the nonlinear relaxation time of the population density as a function of the Cauchy noise intensity was found.

ACKNOWLEDGMENTS

Authors acknowledge the financial support by MIUR.

REFERENCES

Acedo L. 2006. A second-order phase transition in the complete graph stochastic epidemic model. *Physica A* 370:613-624.

Agudov NV, Dubkov AA, Spagnolo B. 2003. Escape from a metastable state with fluctuating barrier. *Physica A* 325:144-151.

Agudov NV, Krichigin AV, Valenti D, Spagnolo B. 2010. Stochastic resonance in a trapping overdamped monostable system. *Phys. Rev. E* 81:051123 (8).

Agudov NV, Spagnolo B. 2001. Noise-enhanced stability of periodically driven metastable states. *Phys. Rev. E* 64:035102(R)(4).

Ai BQ, Wang XJ, Liu GT, Liu LG. 2003. Correlated noise in a logistic growth model. *Phys. Rev. E* 67:022903(3).

Akeson M, Branton D, Kasianowicz JJ, Brandin E, Deamer DW. 1999. Microsecond Time-scale Discrimination Among Polycytidylic Acid, Polyadenylic Acid, and Polyuridylic Acid as Homopolymers or as Segments Within Single RNA Molecules. *Biophys. J.* 77:3227-3233.

Bagwell GJ, Čokl A, Millar JG. 2008. Characterization and Comparison of Substrate-Borne Vibrational Signals of *Chlorochroa uhleri*, *Chlorochroa ligata*, and *Chlorochroa sayi. Ann. Entomol. Soc. Am.* 101(1):235-246.

Bahar S, Neiman A, Wilkens L, Moss F. 2002. Phase synchronization and stochastic resonance effects in the crayfish caudal photoreceptor. *Phys. Rev. E*, 65:050901(R)(4).

Benzi R, Parisi G, Sutera A, Vulpiani A. 1982. Stochastic resonance in climatic change. *Tellus* 34:10-16.

Benzi R, Sutera A, Vulpiani A. 1981. The mechanism of stochastic resonance. *J. Phys.: Math Gen.* 14:L453-L457.

Bier M, Astumian RD. 1993. Matching a diffusive and a kinetic approach for escape over a fluctuating barrier. *Phys. Rev. Lett.* 71:1649-1652.

Binder K. 1973. Time-Dependent Ginzburg-Landau Theory of Nonequilibrium Relaxation.

Bjørnstad ON, Grenfell BT. 2001. Noisy Clockwork: Time Series Analysis of Population Fluctuations in Animals. *Science* 293:638-643.

Boguna M, Porra JM, Masoliver J, Lindenberg K. 1998. Properties of resonant activation phenomena. *Phys. Rev. E* 57:3990-4002.

Borges M, Jepson PC, Howse PE. 1987. Long-range mate location and close-range courtship behaviour of the green stink bug, *Nezara viridula* and its mediation by sex pheromones. *Entomol. Exp. Appl.* 44:205-212.

Bouché V. 1982. A new instability phenomenon in the Malthus-Verhulst model. *J. Phys. A: Math. Gen.* 15:1841-1848.

Braun HA, Wissing H, Schäfer K, Hirsch MC. 1994. Oscillation and noise determine signal transduction in shark multimodal sensory cells. *Nature* 367:270-273.

Brenig L, Banai N. 1982. Non-linear dynamics of systems coupled with external noise: Some exact results. *Physica D* 5:208-226.

Brumer Y, Michor F, Shakhnovich EI. 2006. Genetic instability and the quasispecies model. *J. Theor. Biol.* 241:216-222.

Bulsara A, Jacobs EW, Zhou EW, Moss F, Kiss L. 1991. Stochastic resonance in a single neuron model: Theory and analog simulation. *J. Theor. Biol.*, 152:531-555.

Calisto H, Bologna M. 2007. Exact probability distribution for the Bernoulli-Malthus-Verhulst model driven by a multiplicative colored noise. *Phys. Rev. E* 75:050103(4).

Chaturvedi S, Gardiner CW, Walls DF. 1976. Exact Fokker-Planck equations from stochastic master equations. *Phys. Lett. A* 57:404-406.

Chialvo DR, Apkarian AV. 1993. Modulated noisy biological dynamics: three examples. *J. Stat. Phys.*, 70:375-391.

Chichigina OA. 2008. Noise with memory as a model of lemming cycles. *Eur. Phys. J. B* 65:347-352.

Ciuchi S, De Pasquale F, Spagnolo B. 1993. Nonlinear relaxation in the presence of an absorbing barrier. *Phys. Rev. E* **47**, 3915-3926 (1993).

Ciuchi S, De Pasquale F, Spagnolo B. 1996. Self-regulation mechanism of an ecosystem in a non-Gaussian fluctuation regime. *Phys. Rev. E* **54**, 706-716.

Čokl A, Virant Doberlet M, McDowell A. 1999. Vibrational directionality in the southern green stink bug, Nezara viridula (L.), is mediated by female song. *Anim. Behav.* 58:1277-1283.

Čokl A, Virant Doberlet M, Stritih N. 2000. The structure and function of songs emitted by southern green stink bugs from Brazil, Florida, Italy and Slovenia. *Physiol. Entomol.* 25:196-205.

Čokl A, Virant Doberlet M. 2003. Communication with substrate-borne signals in small plant-dwelling insects. *Annu. Rev. Entomol.* 48:29-50.

Čokl A, Zorović M, Millar JG. 2007. Vibrational communication along plants by the stink bugs *Nezara viridula* and *Murgantia histrionica*. *Behav. Process.* 75:40-54.

Čokl A, Zorović M, Žunič A, Virant Doberlet M. 2005. Tuning of host plants with vibratory songs of *Nezara viridula* L (Heteroptera: Pentatomidae). *J. Exp. Biol.* 208:1481-1488.

Colazza S, Fucarino A, Peri E, Salerno G, Conti E, Bin F. 2004. Insect oviposition induces volatile emission in herbaceous plants that attracts egg parasitoids. *J. Exp. Biol.* 207:47-53.

Das AK. 1983. A stochastic approach to the freezing of supercooled liquids. *Can. J. Phys.* 61:1046-1049.

Deng J, Schoenbach KH, Buescher ES, Hair PS, Fox PM, Beebe SJ. 2003. The Effects of Intense Submicrosecond Electrical Pulses on Cells. *Biophysical J.* 84:2709-2714.

Derise G, Adam JA. 1990. A generalisation of a solvable model in population dynamics. *J. Phys. A: Math. Gen.* **23**, L727S-L731S.

Doering CR, Gadoua JC. 1992. Resonant activation over a fluctuating barrier. *Phys. Rev. Lett.* 69:2318-2321.

Douglass JK, Wilkens L, Pantazelou E, Moss F. 1993. Noise enhancement of information transfer in crayfish mechanoreceptors by stochastic resonance. *Nature*, 365:337-340.

Duarte JRR, Vermelho MVD, Lyra ML. 2008. Stochastic resonance of a periodically driven neuron under non-Gaussian noise. *Physica A* 387:1446-1454.

Dubkov AA, Agudov NV, Spagnolo B. 2004. Noise-enhanced stability in fluctuating metastable states. *Phys. Rev. E* 69:061103(7).

Dubkov AA, Spagnolo B, Uchaikin VV. 2008. Lévy flights superdiffusion: An introduction. *Int. J. Bifurcat. Chaos* 18:2649-2672.

Dubkov AA, Spagnolo B. 2005. Generalized Wiener process and Kolmogorov's equation for diffusion induced by non-Gaussian noise source. *Fluct. Noise Lett.* 5:L267-L274.

Eigen M, Schuster P. 1979. *The Hypercycle: A Principle of Natural Self-Organization*, (Springer, Berlin).

Eigen M. 1971. Selforganization of matter and the evolution of biological macromolecules. *Naturwissenschaften* 58:465-523.

Feller W. 1971. *An Introduction to Probability Theory and its Applications, Vol. 2* (John Wiley & Sons, Inc., New York).

Fiasconaro A, Spagnolo B. 2009. Stability measures in metastable states with Gaussian colored noise. *Phys. Rev. E* 80:041110(6).

Forrey C, Muthukumar M. 2007. Langevin dynamics simulations of ds-DNA translocation through synthetic nanopores. *J. Chem. Phys.* 127:015102(10).

Freund J, Schimansky-Geier L, Beisner B, Neiman A, Russell D, Yakusheva T, Moss F. 2002 Behavioral stochastic resonance: How the noise from a Daphnia swarm enhances individual prey capture by juvenile paddlefish. *J. Theor. Biol.*, 214:71-83.

Fucarino A. 2003. *Semiochemical relationships in the tritrophic system Leguminous, Nezara viridula (L.) and Trissolcus basalis (Woll.)* (Ph.D. thesis, University of Palermo, Italy).

Gailey PC, Neiman A, Collins JJ, Moss F. 1997. Stochastic Resonance in Ensembles of Nondynamical Elements: The Role of Internal Noise. *Phys. Rev. Lett.* 79:4701-4704.

Gammaitoni L, Hänggi P, Jung P, Marchesoni F. 1998. Stochastic resonance. *Rev. Mod. Phys.* 70:223-287.

Gammaitoni L. 1995. Stochastic resonance and the dithering effect in threshold physical systems. *Phys. Rev. E* 52:4691-4698; Gammaitoni L. 1995. Stochastic resonance in multi-threshold systems. *Phys. Lett. A* 74:315-322.

Gardiner CW, Chaturvedi S. 1977. The Poisson representation. I. A new- technique for chemical master equations. *J. Stat. Phys.* 17:429-468.

Gingl Z, Kiss LB, Moss F. 1995. Non-Dynamical Stochastic Resonance: Theory and Experiments with White and Arbitrarily Coloured Noise. *Europhys. Lett.* 29:191-196.

Giuffrida A, Valenti D, Ziino G, Spagnolo B, Panebianco A. 2009. A stochastic interspecific competition model to predict the behaviour of Listeria monocytogenes in the fermentation process of a traditional Sicilian salami. *Eur. Food Res. Technol.* 228:767-775.

Golec J, Sathananthan S. 2003. Stability analysis of a stochastic logistic model. *Math. Comput. Modell.* 38:585-593.

Gracheva ME, Leburton JP. 2008. Simulation of electrically tunable semiconductor nanopores for ion current/single bio-molecule manipulation. *J. Comput. Electron.* 7:6-9.

Greenwood PE, Müller UU, Ward LM. 2004. Soft threshold stochastic resonance. *Phys. Rev. E* 70:051110(10).

Greenwood PE, Ward LM, Russell DF, Neiman A, Moss F. 2000. Stochastic Resonance Enhances the Electrosensory Information Available to Paddlefish for Prey Capture. *Phys. Rev. Lett.* 84:4773-4776.

Grenfell BT, Wilson K, Finkenstädt BF, Coulson TN, Murray S, Albon SD, Pemberton JM, Clutton-Brock TH, Crawley MJ. 1998. Noise and determinism in synchronized sheep dynamics. Nature 394:674-677.

Halwachs S, Schäfer I, Seibel P, Honscha W. 2009. Antiepileptic drugs reduce efficacy of methotrexate chemotherapy by downregulation of Reduced folate carrier transport activityResistance to MTX chemotherapy by antiepileptic drugs. Leukemia 23:1087-1097.

Herman R, Montroll EW. 1972. A manner of characterizing the development of countries. *Proc. Natl. Acad. Sci. USA* 69:3019-3023.

Higgins CF. 2007. Multiple molecular mechanisms for multidrug resistance transporters. Nature 446:749-757.

Horsthemke W, Lefever R. 1984. *Noise-Induced Transitions: Theory and Applications in Physics, Chemistry and Biology*, (Springer--Verlag, Berlin).

Jackson PJ, Lambert CJ, Mannella R, Martano P, McClintock PVE, Stocks NG. 1989. Relaxation near a noise-induced transition point. *Phys. Rev. A* 40:2875-2878.

Kasianowicz JJ, Brandin E, Branton D, Deamer DW. 1996. Characterization of individual polynucleotide molecules using a membrane channel. Proc. Natl. Acad. Sci. USA 93:13770-13773.

Kiritani K. 1964. The Effect of Colony Size upon the Survival of Larvae of the Southern Green Stink Bug, *Nezara viridula. Jpn. J. Appl. Entomol. Zool.* 8:45-53.

Komarova NL, Wodarz D. 2007. Effect of cellular quiescence on the success of targeted CML therapy. *PLos ONE* 2:e990(9).

Komarova NL, Wodarz D. 2007. Stochastic modeling of cellular colonies with quiescence: An application to drug resistance in cancer. *Theor. Popul. Bio.* 72:523-538.

Korobkova E, Emonet T, Vilar JM, Shimizu TS, Cluzel P. 2004. From molecular noise to behavioural variability in a single bacterium. Nature 428:574-578.

Lathrop DK, Barrall GA, Ervin EN, Keehan MG, Krupka MA, Kawano R, White HS, Hibbs AH. 2009. Escape Dynamics of DNA from a Nanopore under the Influence of an AC Bias. *Biophys. J.* 96:647a (2009).

Leung HK. 1987. Transient properties of a constrained autocatalytic reacting system perturbed by external white noises. *J. Chem. Phys.* 86:6847-6851.

Leung HK. 1988. Critical slowing down near a noise-induced transition point. *Phys. Rev. A* 37:1341-1344.

Lindner B, Ojalvo JG, Neiman A, Schimansky-Geier L. 2004. Effects of noise in excitable systems. *Physics Reports* 392:321-424.

Longtin A, Bulsara A, Moss F. 1991. Time-interval sequences in bistable systems and the noise-induced transmission of information by sensory neurons. *Phys. Rev. Lett.*, 67:656-659.

Longtin A, Chialvo DR. 1998. Stochastic and Deterministic Resonances for Excitable Systems. *Phys. Rev. Lett.* 81:4012-4015.

Lubensky DK, Nelson DR. 1999. Driven polymer translocation through a narrow pore. *Biophys. J.* 77:1824-1838.

Luo KF, Ala-Nissila T, Ying SC, Bhattacharya A. 2008. Sequence Dependence of DNA Translocation through a Nanopore. *Phys. Rev. Lett.* 100:58101-58104.

Makino J, Morita A. 1985. On the Average Value of the Population Derived from the Stochastic Verhulst Equation. *Progr. Theor. Phys.* 73:1264-1267.

Mannella R, Lambert CJ, Stocks NG, McClintock PVE. 1990. Relaxation of nonlinear systems driven by colored noise: An exact result. *Phys. Rev. A* 41:3016-3020.

Mannion JT, Reccius CH, Cross JD, Craighead HG. 2006. Conformational Analysis of Single DNA Molecules Undergoing Entropically Induced Motion in Nanochannels. *Biophys. J.* 90:4538-4545.

Mantegna RN, Spagnolo B, Trapanese M. 2001. Linear and nonlinear experimental regimes of stochastic resonance. *Phys. Rev. E* 63:011101(8).

Mantegna RN, Spagnolo B. 1994. Stochastic resonance in a tunnel diode. *Phys. Rev. E* 49:R1792-R1795.

Mantegna RN, Spagnolo B. 2000. Experimental Investigation of Resonant Activation. *Phys. Rev. Lett.* 84:3025-3028.

Mathis JH, Kiffe TR. 1984. *Stochastic Population Models: A Compartmental Perspective*, (Springer--Verlag, Berlin).

McNeil KJ, Walls DF. 1974. Nonequilibrium phase transitions in chemical reactions. J. Stat. Phys. 10:439-448.

Meller A, Branton D. 2002. Single molecule measurements of DNA transport through a nanopore. *Electrophoresis* 23:2583-2591.

Meller A, Nivon L, Brandin E, Golovchenko JA, Branton D. 2000. Rapid Nanopore Discrimination Between Single Polynucleotide Molecules. *Proc. Natl. Acad. Sci. USA* 97:1079-1084.

Michor F, Iwasa Y, Nowak M. 2006. The age incidence of chronic myeloid leukemia can be explained by a one-mutation model. *Proc. Natl. Acad. Sci. USA* 103:14931-14934.

Montroll EW. 1978. Social dynamics and the quantifying of social forces. *Proc. Natl. Acad. Sci. USA* 75:4633-4637.

Morita A, Makino J. 1986. Simple analytical solution for multiplicative nonlinear stochastic differential equations by a perturbation technique. *Phys. Rev. A* 34:1595--1598 (1986).

Morita A. 1982. An exact expression for the average value of the population governed by the stochastic Verhulst equation. *J. Chem. Phys.* 76:4191-4194.

Moss F, Pierson D, O'Gorman D. 1994. Stochastic resonance: tutorial and update. *Int. J. Bifurcat. Chaos* 4:1383-1397.

Neiman A, Russell D. 2002. Synchronization of Noise-Induced Bursts in Noncoupled Sensory Neurons. *Phys. Rev. Lett.* 88:138103(4).

Nikolaev A, Gracheva M. 2009. Controlled DNA translocation through a nanopore membrane with different electrostatic landscapes. *Biophys. J.* 96:649a.

Nozaki D, Yamamoto Y. 1998. Enhancement of stochastic resonance in a FitzHugh-Nagumo neuronal model driven by colored noise. *Phys. Lett. A* 243:281-287.

Ogata H. 1983. Logistic equations in nonlinear systems. *Phys. Rev. A* 28:2296-2299.

Panja D, Barkema GT. 2008. Passage Times for Polymer Translocation Pulled through a Narrow Pore. *Biophys. J.* 94:1630-1637.

Pankratova EV, Polovinkin AV, Spagnolo B. 2005. Suppression of noise in FitzHugh–Nagumo model driven by a strong periodic signal. *Phys. Lett. A* 344:43-50.

Pannizzi AR. 2000. Suboptimal nutrition and feeding behavior of hemipterans on less preferred plant food sources. *An. Soc. Entomol. Bras.* 29:1-12.

Park PJ, Sung W. 1998. A stochastic model of polymer translocation dynamics through biomembranes. *Int. J. Bifurcat. Chaos* 8:927-931.

Pei X, Bachmann K, Moss F. 1995. The detection threshold, noise and stochastic resonance in the Fitzhugh-Nagumo neuron model. *Phys. Lett. A* 206:61-65.

Pikovsky AS, Kurths J. 1997. Coherence Resonance in a Noise-Driven Excitable System. *Phys. Rev. Lett.* 78:775-778.

Pizzolato N, Fiasconaro A, Persano Adorno D, Spagnolo B. 2010. Resonant activation in polymer translocation: new insights into the escape dynamics of molecules driven by an oscillating field. *Physical Biology*, 7:034001(5).

Pizzolato N, Fiasconaro A, Spagnolo B. 2008 Noise Effects in Polymer Dynamics. *Int. J. Bifurcat. Chaos* 18:2871-2876.

Pizzolato N, Fiasconaro A, Spagnolo B. 2009. Noise driven translocation of short polymers in crowded solutions. *J. Stat. Mech: Theory and Exp.* P01011(10).

Pizzolato N, Valenti D, Persano Adorno D, Spagnolo B. 2009. Evolutionary dynamics of imatinib-treated leukemic cells by stochastic approach. *Cent. Eur. J. Phys.* 7:541-548;

Roeder I, Horn M, Glauche I, Hochhaus A, Mueller MC, Loeffler M. 2006. Dynamic modeling of imatinib-treated chronic myeloid leukemia: functional insights and clinical implications. *Nature Medicine* 12:1181-1184.

Rouse PE. 1953. A Theory of the Linear Viscoelastic Properties of Dilute Solutions of Coiling Polymers. *J. Chem. Phys.* 21:1272-1280.

Russell DF, Wilkens LA, Moss F. 1999. Use of behavioural stochastic resonance by paddle fish for feeding. Nature 402:291-294.

Schlögl F. 1972. *Z. Phys.* Chemical reaction models for phase transition. 253:147-161.

Sigalov G, Comer J, Timp G, Aksimentiev A. 2008. Detection of DNA sequences using an alternating electric field in a nanopore capacitor. *Nano Lett.* 8:56-63.

Spagnolo B, Cirone M, La Barbera A, De Pasquale F. 2002. Noise-induced effects in population dynamics. *J. Phys.: Condens. Mat.* 14:2247-2255.

Spagnolo B, Dubkov AA, Pankratov AL, Pankratova EV, Fiasconaro A, Ochab-Marcinek A. 2007. Lifetime of Metastable States and Suppression of Noise in Interdisciplinary Physical Models *Acta Phys. Pol. B* 38:1925-1950.

Spagnolo B, Fiasconaro A, Valenti D. 2003. Noise induced phenomena in lotka-volterra systems. *Fluct. Noise Lett.* 3:L177-L185.

Spagnolo B, Valenti D, Fiasconaro A. 2004. Noise in ecosystems: a short review. *Math. Biosci. Eng.* **1**, 185-211 (2004).

Stocks NG, Mannella R. 2001. Generic noise-enhanced coding in neuronal arrays. Phys. Rev. E 64:030902(4). Stocks NG. 2001. Information transmission in parallel threshold arrays: Suprathreshold stochastic resonance. *Phys. Rev. E* 63:041114 (9); Stocks NG. 2001. Suprathreshold stochastic resonance: an exact result for uniformly distributed signal and noise. *Phys. Lett. A* 279:308-312; Stocks NG. 2000. Suprathreshold Stochastic Resonance in Multilevel Threshold Systems. *Phys. Rev. Lett.* 84:2310-2314.

Storm AJ, Chen J, Zandbergen H, Dekker C. 2005. Translocation of double-strand DNA through a silicon oxide nanopore. *Phys. Rev. E* 71:51903(10) (2005).

Sundaresan VB, Leo DJ. 2008. Modeling and characterization of a chemomechanical actuator using protein transporter. *Sens. Actuators B: Chem.* 131:384-393.

Suzuki M, Kaneko K, Takesue S. 1982. Critical Slowing Down in Stochastic Processes I. *Prog. Theor. Phys.* 67:1756-1775.

Suzuki M, Takesue S, Sasagawa F. 1982. Critical Slowing Down in Stochastic Processes. II - Noise-Induced Long-Time Tail in Random Growing-Rate Models. *Prog. Theor. Phys.* 68:98-115.

Todd JW. 1989. Ecology and behavior of *Nezara viridula*. *Annu. Rev. Entomol.* 34:273-292.

Tremblay E. 1981. *Entomologia applicata, Vol. 2, parte prima*, (Liguori) 66.

Valenti D, Fiasconaro A, Spagnolo B. 2004. Stochastic resonance and noise delayed extinction in a model of two competing species. *Physica A* 331:477-486.

Vernier PT, Sun Y, Marcu L, Craft CM, Gundersen MA. 2004. Nanoelectropulse-Induced Phosphatidylserine Translocation. *Biophysical J.* 86:4040-4048.

Vilar JM, Gomila G, Rub JM. 1998. Stochastic Resonance in Noisy Nondynamical Systems. *Phys. Rev. Lett.* 81:14-17.

Wannamaker RA, Lipshitz SP, Vanderkooy J. 2000. Stochastic resonance as dithering. *Phys. Rev. E* 61:233-236.

Wiesenfeld K, Pierson D, Pantazelou E, Dames C, Moss F. 1994. Stochastic resonance on a circle. *Phys. Rev. Lett.* 72:2125-2129.

Zhdanov VP. Quantitative modeling of selective lysosomal targeting for drug design. 2008. *Eur. Biophys. J.* 37:1329-1334.

Zimmer C. 1999. Life After Chaos. Science 284:83-86.

Zygadło R. 1996. Kinetics of a Verhulst-type system with nonlinearly coupled noise. *Phys. Rev. E* 54:5964-5969; Zygadło R. 2008. Power-law distribution as a result of asynchronous random switching between Malthus and Verhulst kinetics. *Phys. Rev. E* 77:021130(4).